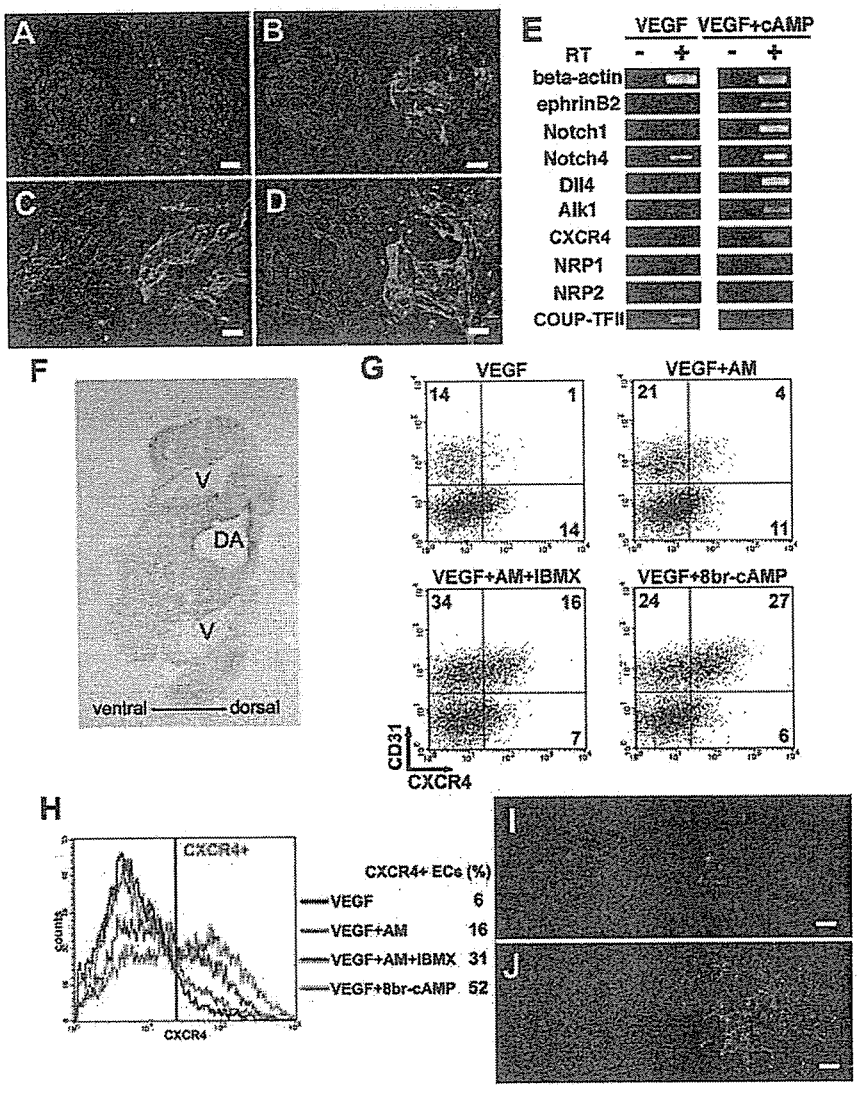

Figure 2. The effect of AM and cAMP on arterial EC induction from VEGFR2$^+$ cells. A to D, Double fluorescent staining for CD31 and ephrinB2 after 3 days of culture of VEGFR2$^+$ cells. Left panels, CD31 (pan-ECs, red) and DAPI (blue). Right panels, EphB4-Fc (ephrinB2$^+$ arterial ECs, green) and DAPI (blue). A, VEGF treatment alone (50 ng/mL). B, VEGF with 10^{-6} mol/L AM. C, VEGF with 10^{-6} mol/L AM and 10^{-4} mol/L IBMX. D, VEGF with 0.5 mmol/L 8bromo-cAMP. Scale bars: 100 μm. E, Reverse-transcription polymerase chain reaction showing mRNA expression of arterial markers (ephrinB2, Notch1, Notch4, Dll4, Alk1, CXCR4, and NRP1) and venous marker (NRP2 and COUP-TFII) in purified ECs induced by VEGF treatment alone or VEGF and 8bromo-cAMP treatment. F, Aortic EC-specific expression of CXCR4 (purple) by in situ hybridization of the isolated aorta-gonad-mesonephros (AGM) region in E11.5 mouse embryo. DA indicates dorsal aorta; V, Cardinal veins. G, Flow cytometry for CD31 and CXCR4 expression. Left upper panel, VEGF treatment alone (50 ng/mL). Right upper panel, VEGF with 10^{-6} mol/L AM. Left lower panel, VEGF with 10^{-6} mol/L AM and 10^{-4} mol/L IBMX. Right lower panel, VEGF with 0.5 mmol/L 8bromo-cAMP. H, Expression profile of CXCR4 in CD31$^+$ ECs by flowcytometry. VEGF treatment alone (blue line), VEGF with 10^{-6} mol/L AM (green line), VEGF with 10^{-6} mol/L AM and 10^{-4} mol/L IBMX (red line), and VEGF with 0.5mmol/L 8bromo-cAMP (orange line) are shown. Percentages of CXCR4$^+$ arterial ECs in total ECs are indicated. I and J, Gross appearance of ephrinB2$^+$ arterial EC induction from VEGFR2$^+$ cells (plated at 2×10^4 cells/cm^2). Left panels, DAPI (blue). Right panels, EphB4-Fc (ephrinB2$^+$ arterial ECs, green). I, VEGF treatment alone (50 ng/mL). J, VEGF with 0.5 mmol/L 8bromo-cAMP. Increase in cell number (DAPI) and substantial arterial EC induction were observed. Scale bars: 400 μm.

8bromo-cAMP and VEGF treatment (Figure 2E). These results indicated that stimulation of cAMP pathway induces arterial ECs.

We further attempted to quantitatively evaluate arterial EC induction at the cellular level. CXCR4, a 7-transmembrane G-protein-coupled receptor, is the receptor of CXCL12 (also known as stromal cell-derived factor-1). Recently, CXCR4 has been reported to be expressed in ECs in the superior mesenteric artery, but not in the superior mesenteric vein, and involved in the formation of arteries in the gastrointestinal tract.[25,30] We examined CXCR4 expression in the mouse embryo by in situ hybridization and found that CXCR4 was detected in ECs of the dorsal aorta but not of cardinal veins in aorta-gonado-mesonephros (AGM) region of E11.5 embryos (Figure 2F). In addition, mRNA expression of CXCR4 was increased in 8bromo-cAMP and VEGF-treated ECs together with other arterial EC markers (Figure 2E), indicating that CXCR4 is another arterial EC marker. FACS analysis using an anti-CXCR4 antibody successfully quantified arterial EC induction by AM or 8bromo-cAMP treatment. Most of ECs induced by VEGF treatment alone (>90% to 95%) were negative for CXCR4. CXCR4$^+$/CD31$^+$ arterial ECs were induced in the presence of AM together with VEGF. Addition of AM with IBMX, or 8bromo-cAMP further increased CXCR4$^+$/CD31$^+$ arterial EC appearance (Figure 2G). Overall, 8bromo-cAMP and VEGF treatment induced ≈5- to 10-fold more CXCR4$^+$ arterial ECs compared with VEGF treatment alone. AM with VEGF treatment showed slight effect on the arterial EC induction. Simultaneous administration of AM and IBMX with VEGF enhanced the arterializing effect of AM (Figure 2H). These results indicated that cAMP signaling mainly contributes to the arterial EC induction. The maximum percentage of arterial ECs within total ECs was increased to ≈60% by 8bromo-cAMP and VEGF (Figure 3F). Addition of 8bromo-cAMP with VEGF led to an increase in total cell number, total EC number, and arterial EC percentage, resulting in ≈70-times increment of induced arterial EC number than those by VEGF alone (Figure 2I and 2J). Higher doses of VEGF (100 to 200 ng/mL) alone or 8bromo-cGMP (0.5 mmol/L) with VEGF

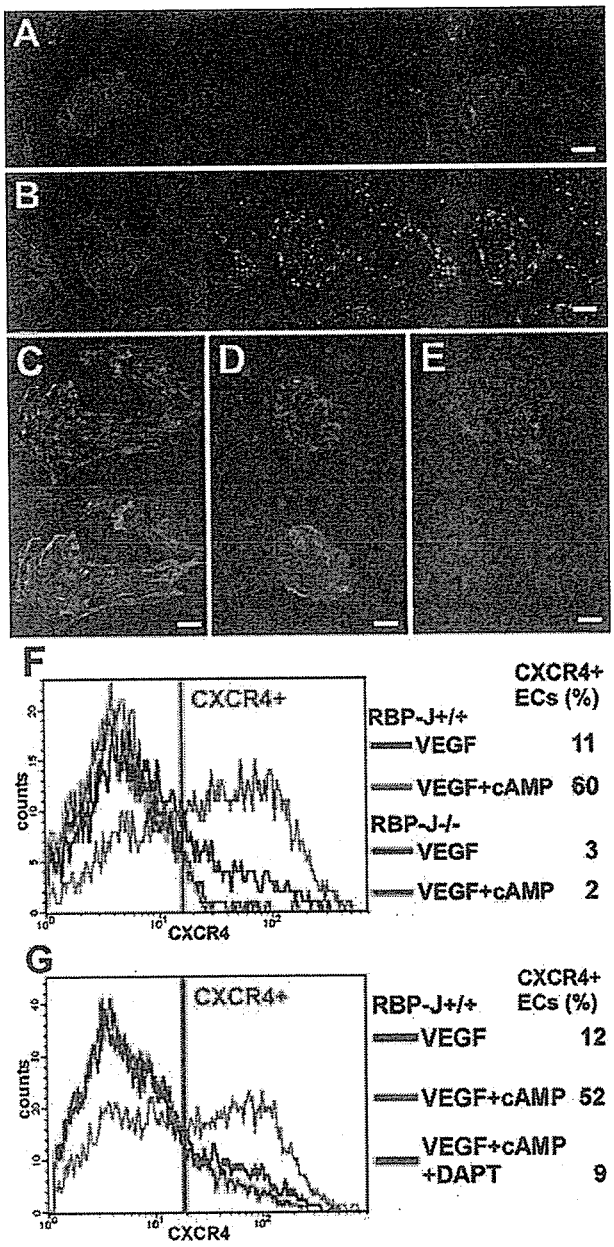

Figure 3. Essential role of Notch signaling in arterial EC induction. A and B, Double fluorescent staining of cleaved Notch intracellular domain (NICD) and CD31 for induced ECs. Left panels, CD31 (pan-ECs, red). Middle panels, Cleaved NICD (green). Right panels, Merged image. A, VEGF treatment alone (50 ng/mL). B, VEGF with 0.5 mmol/L 8bromo-cAMP. Scale Bars: 200 μm. C to E, Double-fluorescent staining of CD31 and ephrinB2 for ECs induced by VEGF with 8bromo-cAMP using RBP-J–deficient ES cells. Upper panels, CD31 (pan-ECs, red) and DAPI (blue). Lower panels, EphB4-Fc (ephrinB2$^+$ arterial ECs, green) and DAPI (blue). C, RBP-J$^{+/+}$ ES cells. D, RBP-J$^{+/-}$ ES cells. E, RBP-J$^{-/-}$ ES cells. Scale bars: 100 μm. F and G, Expression profile of CXCR4 in CD31$^+$ ECs. F, Blue and green lines: RBP-J$^{+/+}$ cells. VEGF treatment alone (blue line), VEGF with 0.5 mmol/L 8bromo-cAMP (green line). Red and orange lines: RBP-J$^{-/-}$ cells. VEGF alone (red line), VEGF with 0.5 mmol/L 8bromo-cAMP (orange line). Percentages of CXCR4$^+$ arterial ECs in total ECs are indicated. G, RBP-J$^{+/+}$ cells. VEGF treatment alone (blue line), VEGF with 0.5 mmol/L 8bromo-cAMP (green line). VEGF with 8bromo-cAMP and 2.5 μmol/L DAPT (red line).

Single-Cell Analysis of VEGFR2$^+$ Cell Culture

	VEGF Alone	VEGF With 8bromo-cAMP
Total colony, n (per every 100 sequential wells)	5.62±1.74 (n=16)	16.0±6.06 (n=11)*
EC-including colony, n (per every 10 sequential colonies)	3.40±2.20 (n=15)	7.00±1.70 (n=19)*
AEC-including colony, n (per every 10 sequential colonies)	1.27±1.10 (n=15)	3.63±1.30 (n=19)*
AEC number (per each AEC-including colony)	1.69±0.87 (n=16)	4.51±2.77 (n=76)*

*P<0.01 vs VEGF alone.
AEC indicates arterial endothelial cell; EC, endothelial cell.

treatment did not show arterial EC induction. Administration of iloprost (10^{-7} to 10^{-5} mol/L), an analogue of prostaglandin-I2 that elevates intracellular cAMP in mature ECs, showed almost no arterial inducing effect even with VEGF treatment (data not shown). These results indicated that AM/cAMP signaling is a novel potent and specific inducer of arterial ECs from vascular progenitor cells.

To further evaluate the mechanism of AM/cAMP-stimulated arterial EC induction, we performed single-cell culture of VEGFR2$^+$ cells. Colonies obtained from single VEGFR2$^+$ cells were counted and evaluated by staining for CD31, ephrinB2, and DAPI (Table). VEGF and 8bromo-cAMP treatment significantly increased the total number of colonies that appeared, number of EC-including colonies, and arterial EC-including colonies in appeared colonies, and arterial EC numbers in each arterial EC-including colony than VEGF alone. These results suggest that cAMP increased survival of VEGFR2$^+$ progenitor cells, differentiation of ECs and arterial ECs from progenitor cells that survived, and proliferation of arterial ECs. cAMP, thus, should be involved in multi steps of arterial EC differentiation processes.

We then examined the role of Notch signaling in arterial EC induction in this system. Activation of Notch on ligand binding is accompanied by proteolytic processing that releases intracellular domain of Notch (NICD) from the membrane. The NICD then translocates into the nucleus and associates with RBP-J, a DNA-binding protein, to form a transcriptional activator, which turns on transcription of a set of target genes.[31] First, we examined Notch activation by cAMP treatment with immunostaining of cleaved NICD. Whereas Notch signal was not activated in most of ECs induced by VEGF alone (Figure 3A), administration of 8bromo-cAMP together with VEGF clearly induced nuclear localization of cleaved NICD in ECs, indicating that stimulation of cAMP pathway can activate Notch signaling in differentiating ECs (Figure 3B). cAMP is, thus, found to be a novel signaling pathway that interacts with and activates Notch signaling in EC lineages. Then, we performed a loss-of-function study using RBP-J–deficient ES cells that lack Notch signaling activation.[20] VEGFR2$^+$ cells derived

from RBP-J$^{+/+}$, RBP-J$^{+/-}$, or RBP-J$^{-/-}$ ES cells were sorted and re-cultured with VEGF in the presence of 8bromo-cAMP. Arterial EC induction observed in RBP-J$^{+/+}$ (Figure 3C) or RBP-J$^{+/-}$ ES cells (Figure 3D) was completely abolished in RBP-J$^{-/-}$ ES cells (Figure 3E). FACS analysis using CXCR4 further demonstrated that induction of CXCR4^{+} arterial ECs observed in RBP-J$^{+/+}$ was completely abolished in RBP-J$^{-/-}$ ES cells (Figure 3F). Similarly, administration of γ-secretase inhibitor, DAPT (2.5μmol/L), which inhibits proteolytic processing of Notch to activate its signaling, to VEGFR2^{+} cell culture also completely blocked the arterial EC induction (Figure 3G). These results indicate that Notch signaling is essential for arterial EC induction in this ES cell system, and correlates with previous reports in zebrafish[32,33] and mouse[34,35] genetic animal models.

Next, we examined the effect of a gain-of-function of Notch in arterial EC induction. We used an ES cell line NERT$^{\Delta OP}$-7,[21] in which signaling of the activated intracellular domain of murine Notch1 can be regulated using an OHT-inducible system.[22] NERT$^{\Delta OP}$-7 ES cell-derived VEGFR2^{+} cells were sorted and re-cultured with VEGF in the presence or absence of OHT. In the absence of OHT, NERT protein was located mainly in the cytoplasm of induced CD31^{+} ECs and other cell types (supplemental Figure IA, available online at http://atvb.ahajournals.org). After addition of OHT, NERT protein translocated to the nucleus (supplemental Figure IB). Notch signal activation in VEGF-induced ECs was evaluated by FACS using NERT$^{\Delta OP}$-7/Hes-GFP cells carrying HES promoter-driven GFP gene (supplemental Figure IC). Addition of 8bromo-cAMP induced endogenous Notch activation in ECs, correlating with our previous results shown in Figure 3A and 3B. OHT treatment showed stronger Notch signal activation through NERT protein than 8bromo-cAMP treatment. Simultaneous stimulation by 8bromo-cAMP and OHT additionally enhanced Notch activation in induced ECs. These results indicate that NERT$^{\Delta OP}$-7 cell system can successfully induce Notch signal activation in differentiating ES cells. NERT$^{\Delta OP}$-7 cell-derived ECs induced by VEGF alone were negative for ephrinB2 (Figure 4A). Unexpectedly, hardly any arterial ECs appeared after Notch activation with OHT, even when co-stimulated with VEGF (Figure 4B). Although ephrin-B2^{+} arterial ECs were successfully induced by VEGF with 8bromo-cAMP (Figure 4C), no apparent effect of OHT was observed on the cAMP-stimulated arterial EC induction with ephrinB2 staining (Figure 4D). FACS analysis further demonstrated that activation of Notch signaling by OHT failed to induce CXCR4^{+} arterial ECs and, moreover, activation of Notch signaling with OHT did not affect, or often reduced, cAMP-induced CXCR4^{+} arterial EC induction (Figure 4E). These results indicate that Notch signal is not sufficient or at least aberrant activation of Notch is not beneficial, for arterial EC induction. This is compatible with the previous in vivo study using activated Notch4-transgenic mice in that activation of Notch signaling in embryonic endothelium led to disorganized vascular networks but did not document arterial induction.[36]

Taken together, VEGF appears essential for EC differentiation from VEGFR2^{+} cells, and venous ECs can be induced by VEGF alone. For arterial EC induction, however, VEGF and Notch signaling is essential but not sufficient. AM/cAMP pathway can activate Notch signaling, and is another important signaling to induce arterial ECs. Coordinated signaling of VEGF, Notch, and cAMP is the combination that composes a sufficient condition to constructively induce arterial ECs from vascular progenitor cells.

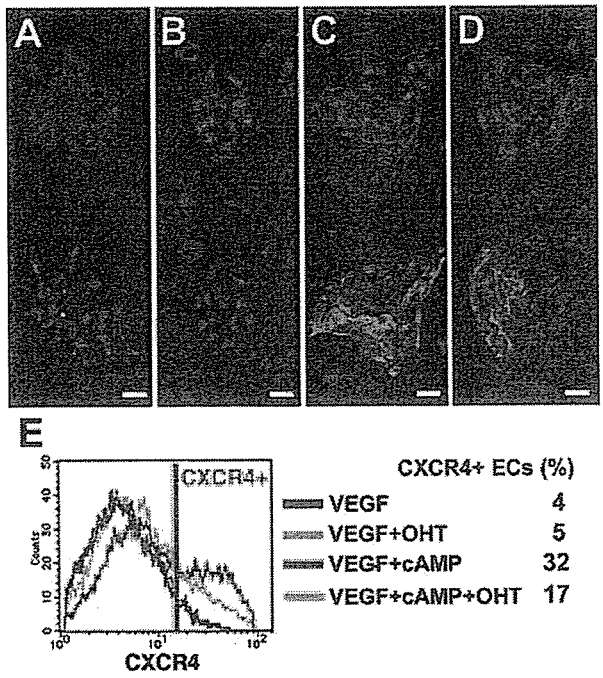

Figure 4. Effects of activated Notch on arterial EC induction from VEGFR2^{+} cells. A-D, Double-fluorescent staining of CD31 and ephrinB2 for induced ECs using NERT$^{\Delta OP}$-7 ES cells. Upper panels, CD31 (pan-ECs, red) and DAPI (blue). Lower panels, EphB4-Fc (ephrinB2^{+} arterial ECs, green) and DAPI (blue). A, VEGF treatment alone (50 ng/mL). B, VEGF and 150 nmol/L OHT. C, VEGF and 0.5 mmol/L 8bromo-cAMP. D, VEGF, 0.5mmol/L 8bromo-cAMP, and 150 nmol/L OHT. Scale bars: 100 μm. E, Expression profile of CXCR4 in CD31^{+} ECs. VEGF alone (blue line), VEGF and OHT (green line), VEGF and 8bromo-cAMP (red line), and VEGF, 8bromo-cAMP, and OHT (orange line) are shown. Percentages of CXCR4^{+} arterial ECs in total ECs are indicated.

Discussion

Our findings provide the first demonstration to our knowledge of arterial and venous EC induction from ES cells by constructively reproducing endothelial differentiation processes in vitro. Here we showed that cAMP and AM play specific roles in EC differentiation, especially for arterial EC induction, from VEGFR2^{+} vascular progenitors. We have shown that AM enhances proliferation and migration of cultured ECs and can promote angiogenesis in gel plug assays in vivo.[37] Recently, AM was reported to enhance angiogenic potency of bone marrow cell transplantation.[38] AM should be a novel potent candidate for an endogenous ligand for EC differentiation as well as arterial EC induction.

Our results showed that stimulation of cAMP pathway can activate Notch signaling in EC lineage. To date, little evidence of Notch activation by cAMP pathway has been reported. In neuronal cells, cAMP-response element-binding protein increased expression of presenilin-1, a component of

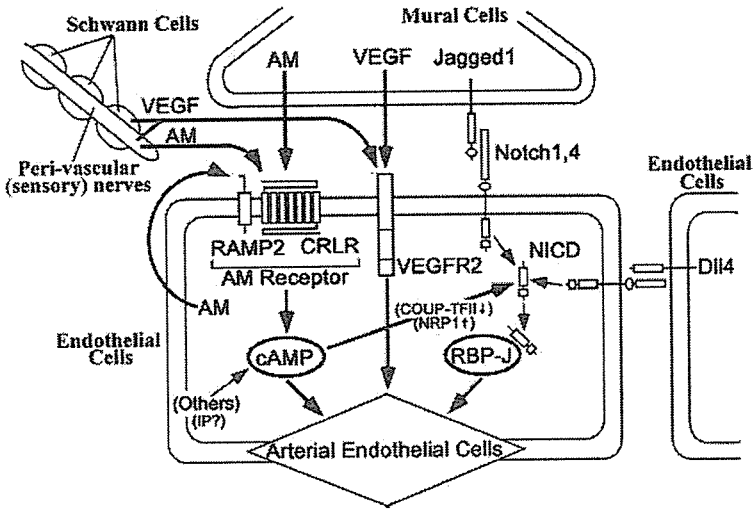

Figure 5. Cellular and molecular mechanisms of arterial EC induction. Putative autocrine/paracrine system for arterial induction in vascular wall. Signals for arterial induction, VEGF, Notch, and AM/cAMP components exist in the vascular wall. VEGFR2, AM receptor complex, RAMP2 and CRLR, and Notch1 and 4 are expressed in ECs. However, their ligands, VEGF, AM, and Jagged1 are expressed in mural cells (MCs). Moreover, AM is expressed in ECs and perivascular nerves. VEGF is produced from peripheral sensory nerves and Schwann cells. Notch ligands, Dll4, and Jagged1 are expressed in arterial ECs. These autocrine/paracrine signals among ECs, MCs, and other perivascular tissues should coordinately regulate the arterial induction and maintenance.

γ-secretase, through transcriptional activation.[39] A similar mechanism may contribute in EC and EC progenitors to induce Notch activation. Recently, COUP-TFII has been reported to repress Notch signaling through suppressing NRP1 expression to maintain vein identity.[28] Administration of 8bromo-cAMP did not increase mRNA expression of Notch ligands (ie, jagged1, 2, Delata-like1, 3, 4) in surrounding mural cells (data not shown), but suppressed COUP-TFII and increased NRP1 expression in ECs. These results suggest that cAMP pathway may activate Notch signaling through the suppression of COUP-TFII expression. cAMP pathway, thus, may regulate the determination of cell fates between arterial and venous ECs. Although Dll4 and Notch signaling were reported to be growth-suppressive on mature ECs through downregulation of VEGFR2 and NRP1 expression,[40] forced Notch activation with OHT did not affect on VEGFR2 and NRP1 mRNA expression in differentiating ECs (data not shown). Notch signaling may possess differentiation stage-specific roles in EC differentiation and proliferation. Precise molecular interactions among these pathways should be further investigated to figure out the whole scheme of arterial-venous specification.

In the vascular wall, VEGFR2, Notch1 and 4, and AM receptor complex, CRLR, RAMP-2 and -3, are expressed in ECs.[5,6] On the other hand, their ligands, VEGF, Jagged1, and AM, are expressed in MCs.[8,41,42] Dll4 and AM are also expressed in ECs. We confirmed AM mRNA expression in ES cell-derived ECs and MCs, and RAMP-2 and CRLR mRNA in ECs by reverse-transcription polymerase chain reaction analysis. Low-level expression of prostaglandin-I2 receptor mRNA was also observed in ECs (data not shown). Moreover, peripheral sensory nerve and Schwann cell-derived VEGF are reported to be involved in arterial EC induction.[43] AM is demonstrated to be expressed in perivascular nerves in the rat mesenteric artery.[44] The autocrine/paracrine cross-talk of VEGF, Notch, and AM/cAMP signaling between ECs and MCs, and signals from other perivascular tissues, should coordinately regulate vascular development including the induction and maintenance of the arterial structures (Figure 5). Combinatory signaling of VEGF, Notch, and cAMP may mimic these arterial-inducing machineries in vivo to achieve constructive induction of arterial ECs from vascular progenitor cells in vitro.

Our constructive approach has successfully provided a novel understanding for the mechanisms of arterial EC differentiation. This study, thus, would provide a potent novel strategy as constructive developmental biology to dissect cell differentiation processes and contribute to regenerative medicine.

Acknowledgments

We thank Dr Ohtsuka and Dr Kagayama for Hes promoter gene constructs. We also thank Drs Takahashi and Hoshino for critical reading of the manuscript.

Sources of Funding

J.K.Y. is supported by grants from the Ministry of Education, Science, Sports, and Culture of Japan, the Ministry of Health, Labor, and Welfare of Japan, and PRESTO JST. U.J. is supported by the Deutsche Forschungsgemeinschaft Priority Program 1109 "Stem Cells" and Sonderforschungsbereich 415 "Signal transduction."

Disclosures

None.

References

1. Carmeliet P. Mechanisms of angiogenesis and arteriogenesis. *Nat Med.* 2000;6:389–395.
2. Sato TN. Vascular development: molecular logic for defining arteries and veins. *Curr Opin Hematol.* 2003;10:131–135.
3. Wang HU, Chen ZF, Anderson DJ. Molecular distinction and angiogenic interaction between embryonic arteries and veins revealed by ephrin-B2 and its receptor Eph-B4. *Cell.* 1998;93:741–753.
4. Adams RH, Wilkinson GA, Weiss C, Diella F, Gale NW, Deutsch U, Risau W, Klein R. Roles of ephrinB ligands and EphB receptors in cardiovascular development: demarcation of arterial/venous domains, vascular morphogenesis, and sprouting angiogenesis. *Genes Dev.* 1999; 13:295–306.
5. Lawson ND, Weinstein BM. Arteries and veins: making a difference with zebrafish. *Nat Rev Genet.* 2002;3:674–682.
6. Yamashita JK. Differentiation and diversification of vascular cells from embryonic stem cells. *Int J Hematol.* 2004;80:1–6.
7. Rossant J, Hirashima M. Vascular development and patterning: making the right choices. *Curr Opin Genet Dev.* 2003;13:408–412.
8. Shawber CJ, Kitajewski J. Notch function in the vasculature: insights from zebrafish, mouse and man. *Bioessays.* 2004;26:225–234.

9. Zhong TP, Rosenberg M, Mohideen MA, Weinstein B, Fishman MC. gridlock, an HLH gene required for assembly of the aorta in zebrafish. *Science*. 2000;287:1820–1824.
10. Fischer A, Schumacher N, Maier M, Sendtner M, Gessler M. The Notch target genes Hey1 and Hey2 are required for embryonic vascular development. *Genes Dev*. 2004;18:901–911.
11. Daniel PB, Walker WH, Habener JF. Cyclic AMP signaling and gene regulation. *Annu Rev Nutr*. 1998;18:353–383.
12. Kitamura K, Kangawa K, Kawamoto M, Ichiki Y, Nakamura S, Matsuo H, Eto T. Adrenomedullin: a novel hypotensive peptide isolated from human pheochromocytoma. *Biochem Biophys Res Commun*. 1993;192: 553–560.
13. McLatchie LM, Fraser NJ, Main MJ, Wise A, Brown J, Thompson N, Solari R, Lee MG, Foord SM. RAMPs regulate the transport and ligand specificity of the calcitonin-receptor-like receptor. *Nature*. 1998;393: 333–339.
14. Shimosawa T, Ogihara T, Matsui H, Asano T, Ando K, Fujita T. Deficiency of adrenomedullin induces insulin resistance by increasing oxidative stress. *Hypertension*. 2003;41:1080–1085.
15. Shindo T, Kurihara Y, Nishimatsu H, Moriyama N, Kakoki M, Wang Y, Imai Y, Ebihara A, Kuwaki T, Ju KH, Minamino N, Kangawa K, Ishikawa T, Fukuda M, Akimoto Y, Kawakami H, Imai T, Morita H, Yazaki Y, Nagai R, Hirata Y, Kurihara H. Vascular abnormalities and elevated blood pressure in mice lacking adrenomedullin gene. *Circulation*. 2001;104:1964–1971.
16. Caron KM, Smithies O. Extreme hydrops fetalis and cardiovascular abnormalities in mice lacking a functional adrenomedullin gene. *Proc Natl Acad Sci U S A*. 2001;98:615–619.
17. Nishikawa SI, Nishikawa S, Hirashima M, Matsuyoshi N, Kodama H. Progressive lineage analysis by cell sorting and culture identifies FLK1+VE-cadherin+ cells at a diverging point of endothelial and hemopoietic lineages. *Development*. 1998;125:1747–1757.
18. Yamashita J, Itoh H, Hirashima M, Ogawa M, Nishikawa S, Yurugi T, Naito M, Nakao K, Nishikawa SI. Flk1-positive cells derived from embryonic stem cells serve as vascular progenitors. *Nature*. 2000;408: 92–96.
19. Yurugi-Kobayashi T, Itoh H, Yamashita J, Yamahara K, Hirai H, Kobayashi T, Ogawa M, Nishikawa S, Nishikawa SI, Nakao K. Effective contribution of transplanted vascular progenitor cells derived from embryonic stem cells to adult neovascularization in proper differentiation stage. *Blood*. 2003;101:2675–2678.
20. Schroeder T, Fraser M, Ogawa M, Nishikawa S, Oka C, Bornkamm GW, Nishikawa SI, Honjo T, Just U. Recombination signal sequence-binding protein Jkappa alters mesodermal cell fate decisions by suppressing cardiomyogenesis. *Proc Natl Acad Sci U S A*. 2003;100:4018–4023.
21. Schroeder T, Meier-Stiegen F, Schwanbeck R, Eilken H, Nishikawa S, Haler R, Schreiber S, Bornkamm GW, Nishikawa SI, Just U. Activated Notch1 alters differentiation of embryonic stem cells into mesodermal cell lineages at multiple stages of development. *Mech Dev*. In press.
22. Schroeder T, Just U. Notch signalling via RBP-J promotes myeloid differentiation. *EMBO J*. 2000;19:2558–2268.
23. Ohtsuka T, Imayoshi I, Shimojo H, Nishi E, Kageyama R, McConnell SK Visualization of embryonic neural stem cells using Hes promoters in transgenic mice. *Mol Cell Neurosci*. doi 10.1016/j.mcn. 2005.09.006.
24. Yamashita JK, Takano M, Hiraoka-Kanie M, Shimazu C, Peishi Y, Yanagi K, Nakano A, Inoue E, Kita F, Nishikawa SI Prospective identification of cardiac progenitors by a novel single cell-based cardiomyocyte induction. *FASEB J*. 2005;19:1534–1536.
25. Ara T, Tokoyoda K, Okamoto R, Pandelakis AK, Nagasawa T. The role of CXCL12 in the organ-specific process of artery formation. *Blood*. 2005;105:3155–3161.
26. Hippenstiel S, Witzenrath M, Schmeck B, Hocke A, Krisp M, Krüll M, Seybold J, Seeger W, Rascher W, Schütte H, Suttorp N. Adrenomedullin reduces endothelial hyperpermeability. *Circ Res*. 2002;91:618–625.
27. Fuller T, Korff T, Kilian A, Dandekar G, Augustin HG. Forward EphB4 signaling in endothelial cells controls cellular repulsion and segregation from ephrinB2 positive cells. *J Cell Sci*. 2003;116:2461–2470.
28. You LR, Lin FJ, Lee CT, DeMayo FJ, Tsai MJ, Tsai SY. Suppression of Notch signaling by the COUP-TFII transcription factor regulates vein identity. *Nature*. 2005;435:98–104.
29. Herzog Y, Guttmann-Raviv N, Neufeld G. Segregation of arterial and venous markers in subpopulations of blood islands before vessel formation. *Dev Dyn*. 2005;232:1047–1055.
30. Tachibana K, Hirota S, Iizasa H, Yoshida H, Kawbata K, Kataoka Y, Kitamura Y, Matsushima K, Yoshida N, Nishikawa SI, Kishimoto T, Nagasawa T. The chemokine receptor CXCR4 is essential for vascularization of the gastrointestinal tract. *Nature*. 1998;393:591–594.
31. Mumm JS, Kopan R. Notch signaling: from the outside in. *Dev Biol*. 2000;228:151–165.
32. Zhong TP, S. Childs, J.P. Leu, Fishman. MC. Gridlock signalling pathway fashions the first embryonic artery. *Nature*. 2001;414: 216–220.
33. Lawson ND, Scheer N, Pham VN, Kim CH, Chitnis AB, Campos-Ortega JA, Weinstein BM. Notch signaling is required for arterial-venous differentiation during embryonic vascular development. *Development*. 2001; 128:3675–3683.
34. Duarte A, Hirashima M, Benedito R, Trindade A, Diniz P, Bekman E, Costa L, Henrique D, Rossant J. Dosage-sensitive requirement for mouse Dll4 in artery development. *Genes Dev*. 2004;18:2474–2478.
35. Krebs LT, Shutter JR, Tanigaki K, Honjo T, Stark KL, Gridley T. Haploinsufficient lethality and formation of arteriovenous malformations in Notch pathway mutants. *Genes Dev*. 2004;18:2469–2473.
36. Uyttendaele H, Ho J, Rossant J, Kitajewski J. Vascular patterning defects associated with expression of activated Notch4 in embryonic endothelium. *Proc Natl Acad Sci U S A*. 2001;98:5643–5648.
37. Miyashita K, Itoh H, Sawada N, Fukunaga Y, Sone M, Yamahara K, Yurugi-Kobayashi T, Park K, Nakao K. Adrenomedullin provokes endothelial Akt activation and promotes vascular regeneration both in vitro and in vivo. *FEBS Lett*. 2003;544:86–92.
38. Iwase T, Nagaya N, Fujii T, Itoh T, Ishibashi-Ueda H, Yamagishi M, Miyatake K, Matsumoto T, Kitamura S, Kangawa K. Adrenomedullin enhances angiogenic potency of bone marrow transplantation in a rat model of hindlimb ischemia. *Circulation*. 2005;111:356–362.
39. Mitsuda N, Ohkubo N, Tamatani M, Lee YD, Taniguchi M, Namikawa K, Kiyama H, Yamaguchi A, Sato N, Sakata K, Ogihara T, Vitek MP, Tohyama M. Activated cAMP-response element-binding protein regulates neuronal expression of presenilin-1. *J Biol Chem*. 2001;276: 9688–9698.
40. Williams CK, Li JL, Murga M, Harris AL, Tosato G. Up-regulation of the Notch ligand Delta-like 4 inhibits VEGF-induced endothelial cell function. *Blood*. 2006;107:931–939.
41. Darland DC, Massingham LJ, Smith SR, Piek E, Saint-Geniez M, D'Amore PA. Pericyte production of cell-associated VEGF is differentiation-dependent and is associated with endothelial survival. *Dev Biol*. 2003;264:275–288.
42. Montuenga LM, Mariano K, Prentice MA, Cuttitta F, Jakowlew SB. Coordinate expression of transforming growth factor-beta1 and adrenomedullin in rodent embryogenesis. *Endocrinology*. 1998;139: 3946–3957.
43. Mukouyama YS, Shin D, Britsch S, Taniguchi M, Anderson DJ. Sensory nerves determine the pattern of arterial differentiation and blood vessel branching in the skin. *Cell*. 2002;109:693–705.
44. Hobara N, Nakamura A, Ohtsuka A, Narasaki M, Shibata K, Gomoita Y, Kawasaki H. Distribution of adrenomedullin-containing perivascular nerves in the rat mesenteric artery. *Peptides*. 2004;25:589–599.

Am J Physiol Endocrinol Metab 290: E583–E590, 2006.
First published October 25, 2005; doi:10.1152/ajpendo.00395.2005.

Low-intensity contraction activates the α1-isoform of 5′-AMP-activated protein kinase in rat skeletal muscle

Taro Toyoda,[1] Satsuki Tanaka,[2] Ken Ebihara,[2] Hiroaki Masuzaki,[2] Kiminori Hosoda,[2] Kenji Sato,[3] Tohru Fushiki,[1] Kazuwa Nakao,[2] and Tatsuya Hayashi[4]

[1]Laboratory of Nutrition Chemistry, Division of Food Science and Biotechnology, Graduate School of Agriculture, Kyoto University; [2]Department of Medicine and Clinical Science, Graduate School of Medicine, Kyoto University; [3]Laboratory of Food Science, Department of Food Sciences and Nutritional Health, Kyoto Prefectural University; and [4]Laboratory of Sports and Exercise Medicine, Graduate School of Human and Environmental Studies, Kyoto University, Kyoto, Japan

Submitted 23 August 2005; accepted in final form 20 October 2005

Toyoda, Taro, Satsuki Tanaka, Ken Ebihara, Hiroaki Masuzaki, Kiminori Hosoda, Kenji Sato, Tohru Fushiki, Kazuwa Nakao, and Tatsuya Hayashi. Low-intensity contraction activates the α1-isoform of 5′-AMP-activated protein kinase in rat skeletal muscle. *Am J Physiol Endocrinol Metab* 290: E583–E590, 2006. First published October 25, 2005; doi:10.1152/ajpendo.00395.2005.—Skeletal muscle expresses two catalytic subunits, α1 and α2, of the 5′-AMP-activated protein kinase (AMPK), which has been implicated in contraction-stimulated glucose transport and fatty acid oxidation. Muscle contraction activates the α2-containing AMPK complex (AMPKα2), but this activation may occur with or without activation of the α1-containing AMPK complex (AMPKα1), suggesting that AMPKα2 is the major isoform responsible for contraction-induced metabolic events in skeletal muscle. We report for the first time that AMPKα1, but not AMPKα2, can be activated in contracting skeletal muscle. Rat epitrochlearis muscles were isolated and incubated in Krebs-Ringer bicarbonate buffer containing pyruvate. In muscles stimulated to contract at a frequency of 1 and 2 Hz during the last 2 min of incubation, AMPKα1 activity increased twofold and AMPKα2 activity remained unchanged. Muscle stimulation did not change the muscle AMP concentration or the AMP-to-ATP ratio. AMPK activation was associated with increased phosphorylation of Thr^{172} of the α-subunit, the primary activation site. Muscle stimulation increased the phosphorylation of acetyl-CoA carboxylase (ACC), a downstream target of AMPK, and the rate of 3-*O*-methyl-D-glucose transport. In contrast, increasing the frequency (≥5 Hz) or duration (≥5 min) of contraction activated AMPKα1 and AMPKα2 and increased AMP concentration and the AMP/ATP ratio. These results suggest that *1*) AMPKα1 is the predominant isoform activated by AMP-independent phosphorylation in low-intensity contracting muscle, *2*) AMPKα2 is activated by an AMP-dependent mechanism in high-intensity contracting muscle, and *3*) activation of each isoform enhances glucose transport and ACC phosphorylation in skeletal muscle.

exercise; twitch; glucose transport; acetyl-coenzyme A carboxylase; β-oxidation

EXERCISE TRIGGERS AN INCREASE in glucose and fatty acid utilization in contracting muscle. 5′-AMP-activated protein kinase (AMPK) is an important signaling intermediary in this increased use of substrates. AMPK activation leads to contraction-stimulated glucose transport in skeletal muscle (21, 34) and is thought to be involved in the regulation of fatty acid oxidation by phosphorylation of acetyl-CoA carboxylase (ACC) (49). Phosphorylation of AMPK by its upstream kinase AMPK kinase (AMPKK) increases the activity of AMPK (26, 47). AMPK activity also increases in response to an increase in AMP concentration or in the AMP-to-ATP ratio (1, 2, 9, 33). Binding of AMP directly activates AMPK through allosteric modification and makes AMPK a better substrate for AMPKK (33). AMPK is a heterotrimeric kinase, consisting of a catalytic α-subunit (1) and two regulatory subunits, β and γ (6). Two distinct α-isoforms (α1, α2) exist in mammals (42), and the α-isoform determines the enzyme characteristics, such as different conditions of activation in contracting muscle.

The α2-containing AMPK complex (AMPKα2) is considered the major AMPK isoform responsible for the metabolic changes in contracting skeletal muscle. A single bout of moderate-intensity exercise at ~70% of maximal O_2 uptake ($\dot{V}O_{2max}$), which increases glucose transport and ACC phosphorylation, significantly activates AMPKα2, but not the α1-containing AMPK complex (AMPKα1), in human vastus lateralis muscle (12, 44, 50). In rat skeletal muscle, electrical stimulation (ES) of the sciatic nerve to produce periodic muscle contractions (46) and voluntary treadmill running exercise (35) increase only AMPKα2 activity, which is accompanied by increased glucose transport and ACC phosphorylation. Whole body AMPKα2 knockout mice exhibit impaired whole body insulin sensitivity and abolished stimulation of glucose transport into skeletal muscle induced by 5-aminoimidazole-4-carboxamide-1-β-D-ribofuranoside (AICAR), an AMPK activator (27). These results suggest that lower-intensity exercise or muscle contraction activates AMPKα2 more than AMPKα1 and that activation of AMPKα2 alone is sufficient to increase glucose transport and ACC phosphorylation. An acute bout of exercise increases the nuclear content of AMPKα2 but not of AMPKα1 (31). These findings indicate the importance of AMPKα2 in contraction-induced metabolic changes in skeletal muscle.

AMPKα1 has also been implicated in skeletal muscle metabolism. Earlier studies suggested that AMPKα1 activity increases only in response to high-intensity exercise, such as a 30-s all-out sprint exercise in humans (3). High-intensity contractions, such as electrically induced tetanic contractions, increase AMPKα1 activity in isolated rat skeletal muscle (35). In contrast, recent reports indicate that AMPKα1 activity also increases in response to moderate-intensity exercise (4, 5). One study reported a small but significant increase in AMPKα1

Address for reprint requests and other correspondence: T. Hayashi, Laboratory of Sports and Exercise Medicine, Graduate School of Human and Environmental Studies, Kyoto University, Yoshida-nihonmatsu-cho, Sakyo-ku, Kyoto, 606-8501, Japan (e-mail: tatsuya@kuhp.kyoto-u.ac.jp).

The costs of publication of this article were defrayed in part by the payment of page charges. The article must therefore be hereby marked "*advertisement*" in accordance with 18 U.S.C. Section 1734 solely to indicate this fact.

when exercise intensity increased from 40 to 60% of $\dot{V}O_{2max}$ in a progressive incremental exercise protocol (4). Repeated higher-intensity exercise at 85% of $\dot{V}O_{2max}$ also increases AMPKα1 activity in humans (5). These reports suggest that AMPKα1 can be activated by exercise at a lower intensity than previously thought necessary.

The pharmacological activation of AMPKα1 increases glucose transport and ACC phosphorylation, suggesting that AMPKα1 is also involved in glucose and fatty acid metabolism (22, 45). We (45) have previously shown that AMPKα1 is activated by hydrogen peroxide (H_2O_2) in isolated rat epitrochlearis muscle and that this is accompanied by increased glucose transport and ACC phosphorylation. Sodium nitroprusside (SNP) stimulates predominantly AMPKα1 activity and enhances glucose transport in isolated rat skeletal muscle (22). In whole body AMPKα1 knockout mice, contraction-induced glucose transport decreases slightly but significantly in the soleus muscle (27), a muscle that normally has an abundance of α1-subunit in wild-type animals (48). Moreover, the protein content of α1-subunit, but not α2-subunit, increases after 3–8 wk of endurance training in human (10, 29) and rat (38) skeletal muscle, and the protein content of α1-subunit is markedly higher in well-trained than in untrained individuals (36). These findings raise the possibility that AMPKα1 may play an important role in exercise-induced metabolic changes in skeletal muscle.

To our knowledge, no one has studied whether increased AMPKα1 activation increases glucose transport and ACC phosphorylation in wild-type skeletal muscle during contraction. In most previous studies, coactivation of AMPKα2 might have obscured the role of AMPKα1 in contracting skeletal muscle. The purpose of this study was to clarify the metabolic role of AMPKα1 in contracting skeletal muscle. We first determined the stimulation parameters that selectively increase the kinase activity of AMPKα1 but not AMPKα2. Because tetanic contractions stimulate both AMPKα1 and AMPKα2, even when the stimulation duration is for 10 s (35), we used "twitch" contractions to precisely manipulate the contraction intensity.

MATERIALS AND METHODS

Experimental animals. Male Sprague-Dawley rats weighing 100 g were purchased from Clea Japan (Tokyo, Japan). Animals were housed in an animal room maintained at 23°C with a 12:12-h light-dark cycle and fed a standard laboratory diet (Certified Diet MF; Oriental Koubo, Tokyo, Japan) and water ad libitum. Rats were fasted overnight before the experiments and were randomly assigned to the experimental groups. All protocols for animal use and euthanasia were reviewed and approved by the Institute of Laboratory Animals, Graduate School of Medicine, Kyoto University, Japan.

Materials. Pyruvate was purchased from Nacalai Tesque (Kyoto, Japan). The SAMS peptide (HMRSAMSGLHLVKRR) was provided by A. Otaka (Graduate School of Pharmaceutical Sciences, Kyoto University) (45). 3-*O*-[methyl-^{3}H]-D-glucose (3-MG) was purchased from American Radiolabeled Chemicals (St. Louis, MO). [γ-^{32}P]ATP and D-[1-^{14}C]mannitol were obtained from NEN Life Science Products (Boston, MA). P81 filter paper was obtained from Whatman International (Maidstone, UK). Protein A-Sepharose CL-4B was from Amersham Biosciences (Uppsala, Sweden). All other reagents were of analytical grade and obtained from Sigma (St. Louis, MO), unless otherwise stated.

Antibodies. AMPK antibodies were raised in rabbit against isoform-specific peptides derived from the amino acid sequences of rat α1 (residues 339–358) or α2 (residues 490–514) (45). Peptides used for immunization were provided by A. Otaka. Immunized sera were used as antibodies.

Muscle treatment. Rat epitrochlearis muscles were treated as described previously, with modifications (21, 45). Rats were killed by cervical dislocation, and the muscles were rapidly removed. When anesthetized, rats were treated with pentobarbital sodium (50 mg/kg body wt ip), and the muscles were isolated either with or without cervical dislocation. Isolated muscles were frozen immediately after isolation or incubated as follows. Both ends of each muscle were tied with sutures (silk 3-0; Natsume Seisakusho, Tokyo, Japan) and the muscles were mounted on an incubation apparatus with the resting tension set to 0.5 g. The buffers were continuously gassed with 95% O_2-5% CO_2 and maintained at 37°C. Muscles were preincubated in 7 ml of Krebs-Ringer bicarbonate buffer (KRB) (in mM: 117 NaCl, 4.7 KCl, 2.5 $CaCl_2$, 1.2 KH_2PO_4, 1.2 $MgSO_4$, 24.6 $NaHCO_3$) containing 2 mM pyruvate (KRBP) for 40 min. The muscles were then incubated for 60 min in KRBP. For the twitch contraction treatments, muscles were stimulated during the last 0.5, 1, 2, 5, and 8 min of the incubation period at various frequencies (0.5–8 Hz) with 0.1-ms square-wave 50-V pulses. For the tetanic contraction treatments, muscles were stimulated during the last 10 min of the incubation period (train rate = 1/min, train duration = 10 s, pulse rate = 100 pulses/s, duration = 0.1 ms, volts = 50 V). The muscles were then used for the measurement of glucose uptake (see *3-MG transport*), or immediately frozen in liquid nitrogen and subsequently analyzed for AMP, ATP (see *Assays for metabolites*), and isoform-specific AMPK activity, or used for Western blot analysis.

Western blotting and isoform-specific AMPK activity assay. Muscles were homogenized in ice-cold lysis buffer (1:40 wt/vol) containing 20 mM Tris·HCl (pH 7.4), 1% Triton X, 50 mM NaCl, 250 mM sucrose, 50 mM NaF, 5 mM sodium pyrophosphate, 2 mM dithiothreitol, 4 mg/l leupeptin, 50 mg/l trypsin inhibitor, 0.1 mM benzamidine, and 0.5 mM phenylmethylsulfonyl fluoride and centrifuged at 20,000 *g* for 40 min at 4°C. For Western blot analysis, denatured lysates (10 μg of protein) were separated on either 7% polyacrylamide gel for phosphorylated AMPK or 5% gel for phosphorylated ACC. Proteins were then transferred to polyvinylidene difluoride membranes (PolyScreen; NEN Life Science Products) at 100 V for 1 h. Membranes were blocked with Block Ace (Yukijirushi Nyugyo, Sapporo, Japan) overnight at 4°C and were then incubated with phosphospecific antibodies directed against AMPKα Thr^{172} (Cell Signaling Technology, Beverly, MA) or against ACC Ser^{79} (Upstate Biotechnology, Lake Placid, NY). The membranes were then washed, reacted with anti-rabbit IgG coupled to peroxidase, and developed with enhanced chemiluminescence reagents according to the manufacturer's instructions (Amersham, Buckinghamshire, UK). The signal on the blot was detected and quantified with a Lumino-Image Analyzer LAS-1000 System (Fuji Photo Film, Tokyo, Japan). For the AMPK activity assay, the supernatants (100 μg of protein) were immunoprecipitated with isoform-specific antibodies directed against the α1 or α2 catalytic subunits of AMPK and protein A-Sepharose beads (21, 45). Immunoprecipitates were washed twice both in lysis buffer and in wash buffer (240 mM HEPES and 480 mM NaCl). Kinase reactions were performed in (in mM) 40 HEPES (pH 7.0), 0.1 SAMS peptide, 0.2 AMP, 80 NaCl, 0.8 dithiothreitol, 5 $MgCl_2$, 0.2 ATP (2 μCi of [γ-^{32}P]ATP), in a final volume of 40 μl for 20 min at 30°C. At the end of the reaction, a 15-μl aliquot was removed and spotted onto Whatman P81 paper. The papers were washed six times in 1% phosphoric acid and once in acetone. ^{32}P incorporation was quantitated with a scintillation counter, and kinase activity was expressed as fold increases relative to the basal samples.

Assays for metabolites. Frozen muscles were homogenized in 0.2 M $HClO_4$ (3:25 wt/vol) in an ethanol-dry ice bath and centrifuged at

20,000 *g* for 2 min at −9°C. To determine the concentration of ATP and its degradation products, the supernatant of the homogenate was neutralized with a solution of 2 N KOH and 0.4 M imidazole and then centrifuged at 20,000 *g* for 2 min at −9°C. The supernatant was filtered through a 0.45-μm pore Cosmonice filter W (Nacalai Tesque) and then analyzed by HPLC (DX300, Dionex, Sunnyvale, CA) equipped with an SPD-10Ai detector (Shimadzu, Kyoto, Japan) and an AS-8020 autoinjector (Tosho, Tokyo, Japan). The filtrate was applied to a COSMOSIL 5PE-MS Packed Column (4.6 × 250 mm; Nacalai Tesque) equilibrated with 20 mM sodium phosphate containing 25 mM *N,N*-diethylethanolamine at 1 ml/min. Elution was monitored at 254 nm.

3-MG transport. To assay 3-MG transport, muscles were transferred to 2 ml of KRB containing 1 mM [^{3}H]3-MG (1.5 μCi/ml) and 7 mM D-[1-^{14}C]mannitol (0.3 μCi/ml) at 30°C and further incubated for 10 min (21). The muscles were then blotted onto filter paper, trimmed, frozen in liquid nitrogen, and stored at −80°C. Frozen muscles were weighed and processed by incubating them in 300 μl of 1 M NaOH at 80°C for 10 min. Digestates were neutralized with 300 μl of 1 M HCl, and particulates were precipitated by centrifugation at 20,000 *g* for 2 min. Radioactivity in aliquots of the digested protein was determined by liquid scintillation counting for dual labels, and the extracellular and intracellular spaces were calculated.

Statistical analysis. Results are presented as means ± SE. Means were compared by one-way analysis of variance followed by post hoc comparison with Dunnett's or Scheffé's test as appropriate. Unpaired *t*-tests were used for comparison as appropriate.

RESULTS

AMPKα1 activity was elevated immediately after isolation and decreased during incubation. To allow the epitrochlearis muscles to recover from the isolating procedure, we first determined the incubation period that stabilizes AMPK activity, as measured in anti-α1 and anti-α2 immunoprecipitates from muscles that had been either frozen immediately after isolation or incubated in KRBP for 60, 100, or 120 min and then frozen. AMPKα1 kinase activity was lower in the incubated muscle than in muscle frozen immediately after isolation (Fig. 1*A*). AMPKα1 activity attained a constant level at 60 min of incubation and did not change afterwards, whereas AMPKα2 activity remained unchanged throughout the incubation period (Fig. 1*A*). We also investigated whether AMPKα1 activity differs between muscles frozen immediately after isolation under anesthesia and muscles incubated for 100 min. Regardless of whether cervical dislocation was or was not performed, AMPKα1 activity was higher in the muscles frozen immediately after isolation under anesthesia than in the incubated muscles; AMPKα2 activity did not differ between conditions (Fig. 1*B*).

ES increased AMPKα1activity in a time- and frequency-dependent manner. Tetanic contraction is a standard procedure to stimulate AMPK activity in isolated skeletal muscle (21, 35). Even a single 10-s tetanic contraction is enough to activate

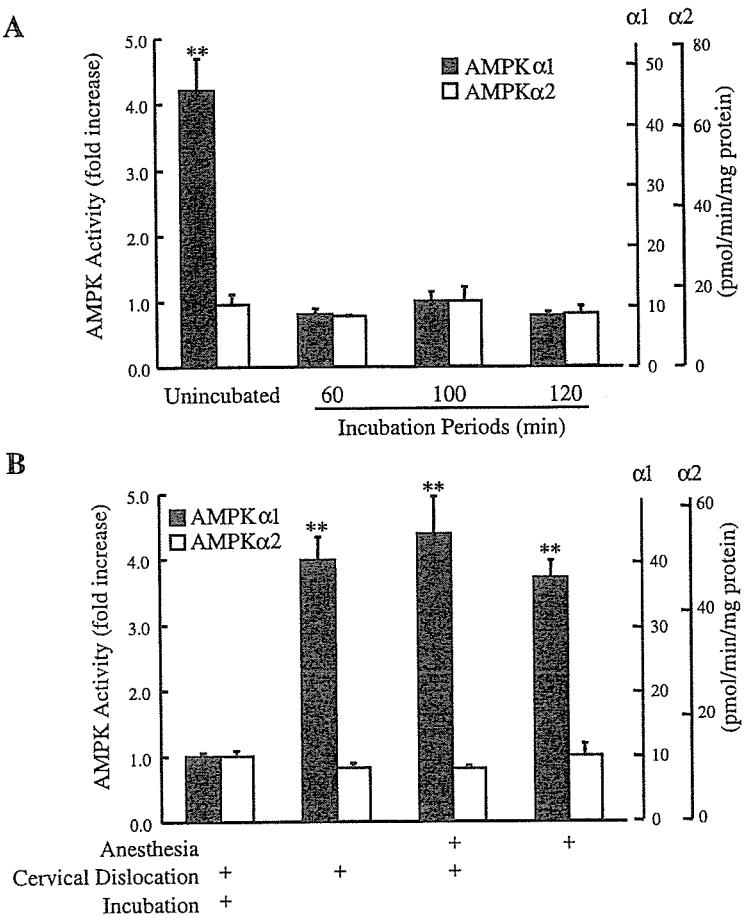

Fig. 1. Incubation decreases 5′-AMP-activated protein kinase (AMPK)α1 activity to a constant level in isolated rat epitrochlearis muscles. *A*: rats were killed by cervical dislocation, and isolated muscles were either frozen immediately after isolation or incubated in Krebs-Ringer bicarbonate buffer containing 2 mM pyruvate (KRBP) for 60, 100, or 120 min and then frozen in liquid nitrogen. *B*: rats were randomly assigned to an anesthetized or a nonanesthetized group. In the anesthetized group, rats were anesthetized with pentobarbital sodium (50 mg/kg body wt ip), and muscles were isolated with or without cervical dislocation. Isolated muscles were frozen immediately after isolation. In the nonanesthetized group, rats were killed by cervical dislocation, and isolated muscles were frozen immediately after isolation or incubated in KRBP for 100 min and then frozen in liquid nitrogen. Isoform-specific AMPK activity was determined in the anti-α1 or anti-α2 subunit of AMPK immunoprecipitates. Fold increases are expressed relative to the activity of muscles incubated for 100 min. Values are means ± SE; $n = 6$ per group. $^{**}P < 0.01$ vs. 100-min incubation group.

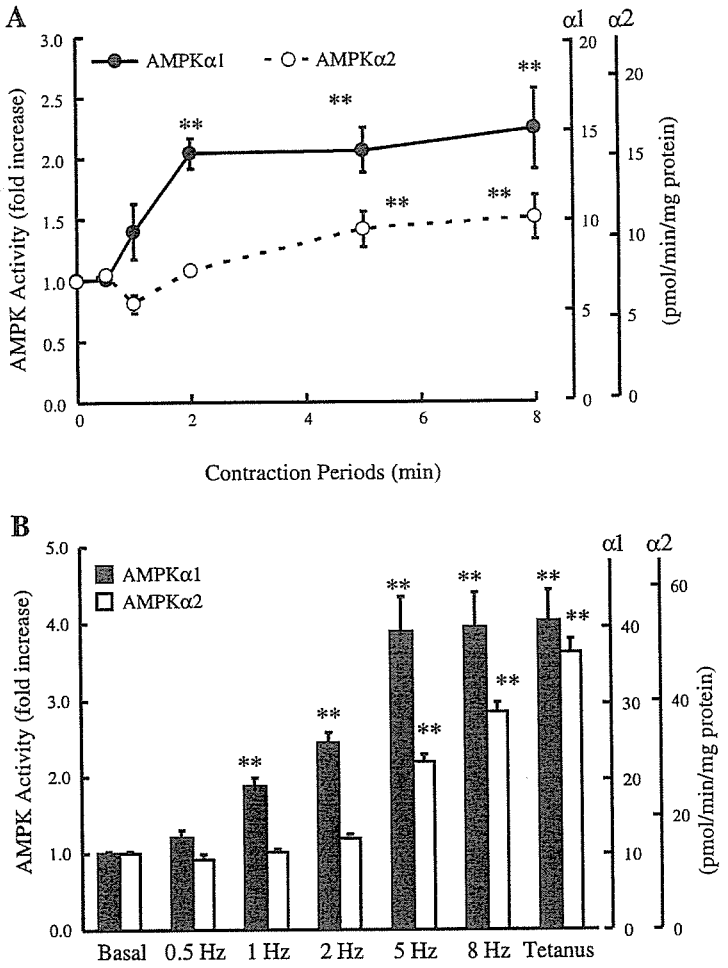

Fig. 2. Low-frequency electrical stimulation (ES) increases predominantly AMPKα1 activity in a time- and contraction frequency-dependent manner in rat epitrochlearis muscles. Isolated muscles were electrically stimulated (50 V) to contract at 1 Hz for the indicated periods (*A*) or at the frequencies indicated for 2 min (*B*). To tetanically contract the muscles, muscles were stimulated for 10 s/min, repeated 10 times. Isoform-specific AMPK activity was determined in anti-α1 or anti-α2 subunit of AMPK immunoprecipitates. Values are means ± SE; n = 9–29 per group. $^{**}P < 0.01$ vs. the 0-min (*A*) or vs. the 0-Hz group (*B*).

both AMPKα1 and AMPKα2 (35). To investigate the time dependency of isoform-specific AMPK activity stimulated by ES at frequencies lower than the tetanic stimulus (100 Hz), isolated epitrochlearis muscles were incubated to stabilize AMPK activity and then stimulated at 1 Hz for various periods. ES at 1 Hz rapidly activated AMPKα1 twofold within 2 min and maintained maximal activity for 2–8 min (Fig. 2*A*). In contrast, AMPKα2 activation required ≥5 min of ES, and the 1.5-fold increase was smaller than that of AMPKα1 ($P < 0.05$; Fig. 2*A*). To determine whether this effect was dependent on stimulation frequency, isolated epitrochlearis muscles were stimulated for 2 min at various frequencies. ES at 1 and 2 Hz activated predominantly AMPKα1, whereas ES at 5 and 8 Hz activated both AMPKα1 and AMPKα2 (Fig. 2*B*). ES at 5 and 8 Hz activated AMPKα1 maximally and to the same degree as tetanic contraction did, about four times the basal level, whereas the activity of AMPKα2 was less than the maximal level achieved at 8 Hz (Fig. 2*B*).

The primary site responsible for AMPK activation is the Thr^{172} residue in both the α1 and α2 catalytic subunits (17, 43). To determine whether the ES-induced activation at 1 and 2 Hz of predominantly AMPKα1 was accompanied by the phosphorylation of Thr^{172}, we measured the degree of phosphorylation of Thr^{172} by use of a phosphospecific antibody in homogenates from muscles that had been stimulated by ES at the two frequencies. Compared with sham-operated muscles, muscles simulated with ES at 1 and 2 Hz exhibited markedly increased phosphorylation of Thr^{172} (Fig. 3).

ES at 1 and 2 Hz changed neither AMP nor the AMP/ATP ratio. To determine whether ES-induced activation of AMPKα1 results from the conventional changes associated with increased AMPK activity (33), we measured AMP concentration and the AMP/ATP ratio after stimulation. ES at 1 and 2 Hz, which activated AMPKα1 but not AMPKα2, did not increase AMP concentration or the AMP/ATP ratio (Fig. 4, *A* and *B*). In contrast, ES at 5 and 8 Hz, and tetanic stimulation, which activated both AMPKα1 and AMPKα2, markedly increased AMP concentration and the AMP/ATP ratio (Fig. 4, *A* and *B*).

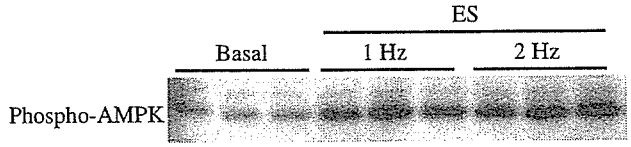

Fig. 3. Low-frequency ES increases phosphorylation of Thr^{172} in the AMPK α-subunit. Isolated muscles were electrically stimulated (50 V) to contract at 1 and 2 Hz for 2 min, and cell lysates were subjected to Western blot analysis with an anti-phosphorylated AMPK antibody.

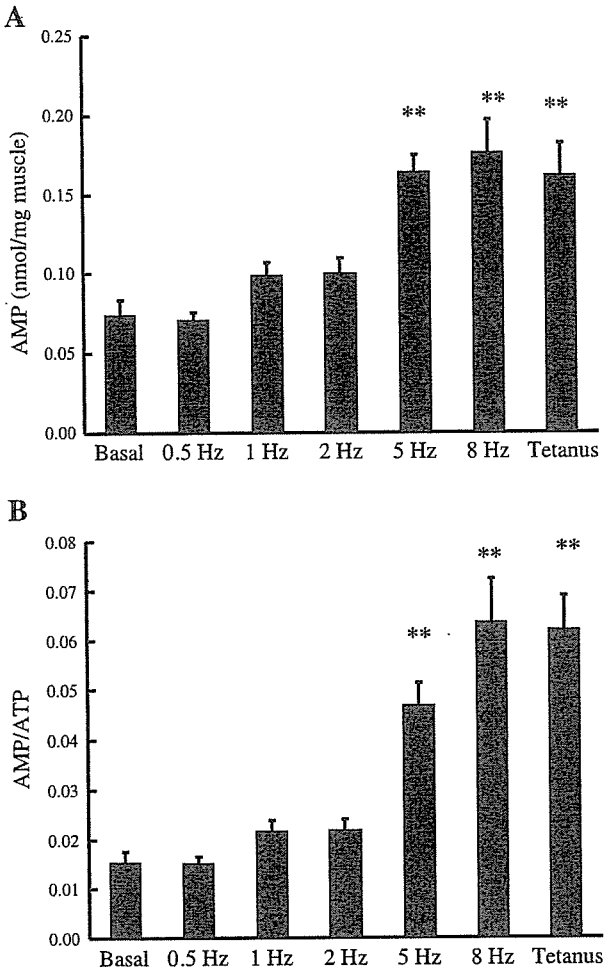

Fig. 4. Adenine nucleotide levels in epitrochlearis muscles treated with low-frequency ES. Isolated muscles were electrically stimulated (50 V) to contract for 2 min at the frequencies indicated. To tetanically contract the muscles, muscles were stimulated for 10 s/min, repeated 10 times. Intracellular AMP concentration (*A*) and ATP concentration were determined by HPLC, and the AMP/ATP ratio (*B*) were calculated. Values are means ± SE; $n = 8–9$ per group. $^{**}P < 0.01$ vs. basal values.

Predominant activation of AMPKα1 by ES at 1 and 2 Hz was associated with increased 3-MG transport and ACC phosphorylation. We next investigated whether ES at 1 and 2 Hz acutely affects glucose transport activity and the phosphorylation state of ACC, a downstream target of AMPK, in skeletal muscle. ES at 1 and 2 Hz increased the transport of the nonmetabolizable glucose analog 3-MG in a frequency-dependent manner (Fig. 5). We used a phosphospecific antibody that recognizes rat ACC1 phosphorylated at Ser^{79} to assess the specific phosphorylation of skeletal muscle ACC, because this site is equivalent to Ser^{79} of ACC1 (15, 37). ES at 1 and 2 Hz increased glucose transport and ACC phosphorylation (Fig. 6).

DISCUSSION

Our data show three novel findings relating to the isoform-specific AMPK profile in skeletal muscle. First, immediately after isolation, the activity of AMPKα1 increased greatly but the activity of AMPKα2 did not change (Fig. 1, *A* and *B*).

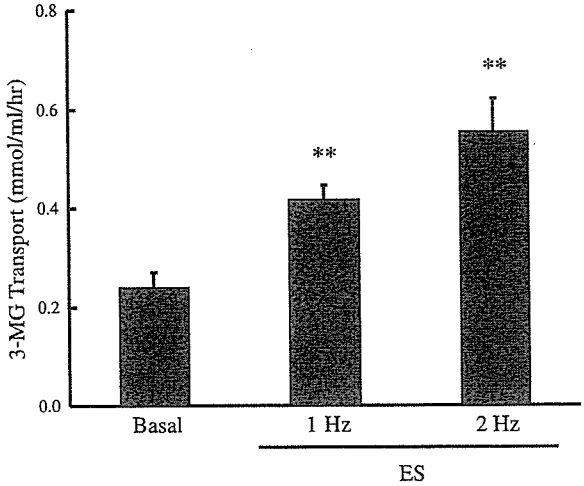

Fig. 5. Electrical stimulation increases 3-*O*-methyl-D-glucose (3-MG) transport in rat epitrochlearis muscles. Isolated muscles were electrically stimulated (1 or 2 Hz at 50 V) to contract for 2 min. Values are means ± SE; $n = 6–10$ per group. $^{**}P < 0.01$ vs. basal values.

Second, muscle contraction induced by ES at 1 and 2 Hz for 2 min activated AMPKα1 but not AMPKα2 (Fig. 2*B*), suggesting that AMPKα1 is more sensitive to low-intensity contraction than AMPKα2 is. Third, contraction-induced AMPKα1 activation was associated with increased glucose transport and ACC phosphorylation (Figs. 5 and 6).

We believe that the marked activation of AMPKα1 immediately after isolation is a post mortem artifact, on the basis of previous studies of liver AMPK (8, 14, 33) showing that, in liver dissected at ambient temperature, 3-hydroxy-3-methylglutaryl-CoA (HMG-CoA) reductase, one of the downstream targets of AMPK, is highly phosphorylated and inactivated (8). In contrast, in liver dissected after cold clamping and homogenized within 10 s after dissection, most HMG-CoA reductase is in an unphosphorylated active form (8), indicating that liver AMPK remains inactive in vivo and is easily activated as a post mortem artifact. Moreover, in freshly isolated rat hepatocytes, AMPK activity increases and then decreases to the expected in vivo level during incubation in oxygenated medium for 60 min (33). Hardie and Carling (14) proposed that rapid cooling is required to preserve the in vivo activation state of AMPK and that incubation in oxygenated medium restores AMPK activity to in vivo levels. Consistent with this proposal, AMPKα1 activation is not observed in muscle after electrically stimulated in situ contraction followed by muscle isolation (40, 46). In contrast, AMPKα1 activation occurs in muscle after electrically stimulated in situ contraction followed by freeze clamping (24).

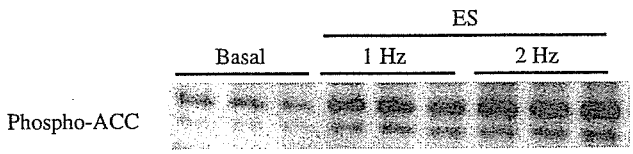

Fig. 6. Low-frequency ES increases phosphorylation of serine in acetyl-CoA carboxylase (ACC). Isolated muscles were electrically stimulated (50 V) to contract at 1 or 2 Hz for 2 min, and cell lysates were subjected to Western blot analysis with an anti-phosphorylated ACC antibody.

We have not identified the critical step of AMPKα1 activation induced by our isolation procedure. Ischemia limits oxygen supply and leads to reduced ATP generation and can activate AMPK (20), and stopping or reducing the blood or oxygen supply to muscles during isolation is one possible cause of AMPKα1 activation. However, hypoxic energy deprivation should activate both AMPKα1 and AMPKα2 (20). In addition, the time needed to freeze the muscle after cervical dislocation was about 30 s, which was about the same amount of time needed to freeze the tissue incubated in oxygenated buffer and then exposed to room air. Furthermore, the activation of AMPKα1 by muscle isolation under anesthesia without cervical dislocation (Fig. 1*B*) shows clearly that cervical dislocation is not a critical step in the activation of AMPKα1. The freezing procedure after incubation is nearly identical to that used after isolation. Thus changes in unidentified factors, such as nervous system input or a soluble factor, might cause the post mortem artifact and increase skeletal muscle AMPKα1 activation during the isolation procedures.

Our finding that low-intensity contraction of skeletal muscle activated mainly AMPKα1 differs from that of previous studies showing predominantly AMPKα2 activation (12, 44, 50). Our use of a different muscle preparation might explain these differences. We measured the AMPK activity of muscles that had been isolated, incubated in KRBP, and then stimulated to contract, whereas previous studies measured AMPK activity of muscles isolated after contraction (12, 44, 50). Because isolation can activate AMPKα1, the actual contraction-induced increase of AMPKα1 activity would not be apparent in the latter protocol. AMPKα1 could also be activated by isolation of both contracted and noncontracted muscles. Our incubation for more than 60 min decreased AMPKα1 activity to a constant level and allowed us to observe the activation of AMPKα1 in low-intensity stimulated contracted muscle.

The finding that AMPKα1 activation was not accompanied by an increase in AMP concentration and the AMP/ATP ratio (Fig. 4, *A* and *B*) suggests that AMPKα1 activation induced by low-intensity contraction is regulated by an AMP-independent mechanism. Although intracellular energy status is an important determinant of AMPK activity (1, 2, 9, 33, 39), recent studies have shown that AMPK is activated by phosphorylation in the absence of changes in the concentration of AMP or ATP or in ADP/ATP or AMP/ATP ratios (11, 22, 32, 45, 51). Our data (Fig. 4) and those of others (22, 45) are consistent in showing that the predominant activation of AMPKα1 is not accompanied by a decrease in intracellular energy status in skeletal muscle. SNP activates AMPKα1 in extensor digitorum longus muscle without depleting ATP (22), and H_2O_2 activates AMPKα1 in rat epitrochlearis muscle without increasing AMP concentration and the AMP/ATP ratio (45). We cannot exclude the possibility that AMPKα1 is activated by the increase in free AMP content, which comprises 0.11–0.50% of the total AMP content (13) and increases markedly in response to muscle contraction (7, 25). Importantly, however, a study using purified AMPK showed that AMPKα2 depends more on AMP activation by the upstream kinase than does AMPKα1 (41). In this context, the absence of AMPKα2 activation in our study also suggests that AMP does not accumulate in muscle and that AMPKα1 activation involves an AMP-independent mechanism (Fig. 2, *A* and *B*). Moreover, we detected parallel increases in AMP concentration and AMPKα2 activity in muscles stimulated by ES at ≥5 Hz (Figs. 2*B* and 4*A*).

Our finding that the predominant AMPKα1 activation is accompanied by phosphorylation of the α-subunit in Thr^{172} suggests that an upstream kinase is involved in AMPKα1 activation by low-intensity contracted muscle (Fig. 3). Two mammalian AMPKKs have been identified: Ca^{2+}/calmodulin-dependent protein kinase kinase (CaMKK) (19, 23) and the LKB1 complex consisting of LKB1 and two regulatory proteins, called Ste20-related adaptor protein and mouse protein 25 (16). In vitro studies have demonstrated that CaMKK is activated by Ca^{2+} and calmodulin but not by AMP (19). In an LKB1-deficient cell line, AMPK can be activated by treatment with mannitol, 2-deoxyglucose, and the Ca^{2+} ionophore ionomycin, but not by the AMP analog AICAR (23). In rat brain slices, depolarization induced by increasing K^+ concentration increases intracellular Ca^{2+} concentration by opening the voltage-gated Ca^{2+} channel and activates AMPK without elevating the AMP/ATP ratio; this activation is blocked by the CaMKK inhibitor STO-609 (18). AMP concentration did not increase in muscles stimulated by ES at 1 and 2 Hz (Fig. 4), suggesting that CaMKK might be responsible for the predominant activation of AMPKα1. In contrast, the LKB1 complex is constitutively active and is not directly activated by AMP, but the binding of AMP to AMPK facilitates the phosphorylation of AMPK by the LKB1 complex (16, 40). Thus the LKB1 complex may depend more on AMP to phosphorylate AMPK than does CaMKK. We cannot discount the possible involvement of yet-to-be-characterized AMPKKs, and further study is needed to clarify the AMPKK that activates predominantly AMPKα1 in low-intensity contracting skeletal muscle.

Our results show that ES at 1 and 2 Hz activates AMPKα1 and increases in the rate of glucose transport and ACC phosphorylation, indicating that AMPKα1, as well as AMPKα2, is involved in contraction-stimulated glucose transport and ACC phosphorylation. Our results are consistent with previous studies showing that low-intensity muscle contraction increases glucose transport and ACC phosphorylation (30, 37). ES at 1 and 2.5 Hz for 5 min increases glucose transport in isolated rat soleus muscles (30). ACC activity decreases after in situ contraction of rat gastrocnemius muscle stimulated by ES at 0.2 and 1 Hz for 5 min via the tibial nerve, and this decreased activity is inversely correlated with the concentration of phosphorylated ACC (37). Moreover, H_2O_2 activates increased glucose transport and ACC phosphorylation associated with AMPKα1 activation (45). SNP increases glucose transport associated with AMPKα1 activation (22). In support of our observations, contraction-induced glucose transport is not reduced by knockout of the α1- or α2-subunit of AMPK but is inhibited by dominant mutants of both isoforms (27, 34).

Our results lead us to hypothesize that *1*) AMPKα1 regulation is more sensitive to physical or physiological stress than AMPKα2 is; *2*) AMPKα1 is the predominant isoform activated by low-intensity contractions; *3*) AMPKα1 activation induced by low-intensity contractions is regulated by an AMP-independent phosphorylation, whereas AMPKα2 activation induced by high-intensity contraction is regulated by AMP-dependent mechanism; and *4*) activation of each isoform enhances glucose transport and ACC phosphorylation in skeletal muscle. Previous data show that low-intensity exercise, even at a level (e.g., 30–40% of $\dot{V}O_{2max}$) previously believed not to activate

AMPK, increases skeletal muscle glucose transport and ACC phosphorylation (4, 28), suggesting the involvement of an AMPK-independent pathway. Our results suggest that AMPKα1 may be activated in these muscles by low-intensity exercise and that measuring the activity may be disturbed by additional activation during isolation. Only during very-high-intensity exercise, when the activation by muscle contraction may exceed that of the isolating stimuli, would AMPKα1 activity be detectable.

In summary, we have demonstrated for the first time that muscle AMPKα1, but not AMPKα2, is activated immediately after isolation. Stabilizing muscle in KRBP followed by low-intensity contraction activates AMPKα1 via phosphorylation without increasing AMP concentration, and it increases glucose transport and ACC phosphorylation. We conclude that low-intensity muscle contraction activates AMPKα1 and leads to enhanced glucose transport and ACC phosphorylation in rat skeletal muscle.

ACKNOWLEDGMENTS

We thank Akira Otaka for providing the purified SAMS peptide and isoform-specific antigen peptides. We are grateful to Kazuo Inoue and Teruo Kawada for suggestions, and to Chikako Wada for secretarial assistance. We also thank the Radioisotope Research Center, Kyoto University, for instrumental support in radioisotope experiments.

GRANTS

This work was supported by research grants from the Japanese Ministry of Education, Science, Sports, and Culture (to T. Hayashi). T. Toyoda was supported by a Research Fellowship of the Japan Society for the Promotion of Science for Young Scientists.

REFERENCES

1. **Carling D, Clarke PR, Zammit VA, and Hardie DG.** Purification and characterization of the AMP-activated protein kinase. Copurification of acetyl-CoA carboxylase kinase and 3-hydroxy-3-methylglutaryl-CoA reductase kinase activities. *Eur J Biochem* 186: 129–136, 1989.
2. **Carling D, Zammit VA, and Hardie DG.** A common bicyclic protein kinase cascade inactivates the regulatory enzymes of fatty acid and cholesterol biosynthesis. *FEBS Lett* 223: 217–222, 1987.
3. **Chen ZP, McConell GK, Michell BJ, Snow RJ, Canny BJ, and Kemp BE.** AMPK signaling in contracting human skeletal muscle: acetyl-CoA carboxylase and NO synthase phosphorylation. *Am J Physiol Endocrinol Metab* 279: E1202–E1206, 2000.
4. **Chen ZP, Stephens TJ, Murthy S, Canny BJ, Hargreaves M, Witters LA, Kemp BE, and McConell GK.** Effect of exercise intensity on skeletal muscle AMPK signaling in humans. *Diabetes* 52: 2205–2212, 2003.
5. **Clark SA, Chen ZP, Murphy KT, Aughey RJ, McKenna MJ, Kemp BE, and Hawley JA.** Intensified exercise training does not alter AMPK signaling in human skeletal muscle. *Am J Physiol Endocrinol Metab* 286: E737–E743, 2004.
6. **Davies SP, Hawley SA, Woods A, Carling D, Haystead TA, and Hardie DG.** Purification of the AMP-activated protein kinase on ATP-gamma-sepharose and analysis of its subunit structure. *Eur J Biochem* 223: 351–357, 1994.
7. **Dudley GA and Terjung RL.** Influence of acidosis on AMP deaminase activity in contracting fast-twitch muscle. *Am J Physiol Cell Physiol* 248: C43–C50, 1985.
8. **Easom RA and Zammit VA.** A cold-clamping technique for the rapid sampling of rat liver for studies on enzymes in separate cell fractions. Suitability for the study of enzymes regulated by reversible phosphorylation-dephosphorylation. *Biochem J* 220: 733–738, 1984.
9. **Ferrer A, Caelles C, Massot N, and Hegardt FG.** Activation of rat liver cytosolic 3-hydroxy-3-methylglutaryl coenzyme A reductase kinase by adenosine 5′ -monophosphate. *Biochem Biophys Res Commun* 132: 497–504, 1985.
10. **Frosig C, Jorgensen SB, Hardie DG, Richter EA, and Wojtaszewski JF.** 5′-AMP-activated protein kinase activity and protein expression are regulated by endurance training in human skeletal muscle. *Am J Physiol Endocrinol Metab* 286: E411–E417, 2004.
11. **Fryer LG, Parbu-Patel A, and Carling D.** The Anti-diabetic drugs rosiglitazone and metformin stimulate AMP-activated protein kinase through distinct signaling pathways. *J Biol Chem* 277: 25226–25232, 2002.
12. **Fujii N, Hayashi T, Hirshman MF, Smith JT, Habinowski SA, Kaijser L, Mu J, Ljungqvist O, Birnbaum MJ, Witters LA, Thorell A, and Goodyear LJ.** Exercise induces isoform-specific increase in 5′ AMP-activated protein kinase activity in human skeletal muscle. *Biochem Biophys Res Commun* 273: 1150–1155, 2000.
13. **Goodman MN and Lowenstein JM.** The purine nucleotide cycle. Studies of ammonia production by skeletal muscle in situ and in perfused preparations. *J Biol Chem* 252: 5054–5060, 1977.
14. **Hardie DG and Carling D.** The AMP-activated protein kinase—fuel gauge of the mammalian cell? *Eur J Biochem* 246: 259–273, 1997.
15. **Hardie DG and Pan DA.** Regulation of fatty acid synthesis and oxidation by the AMP-activated protein kinase. *Biochem Soc Trans* 30: 1064–1070, 2002.
16. **Hawley SA, Boudeau J, Reid JL, Mustard KJ, Udd L, Makela TP, Alessi DR, and Hardie DG.** Complexes between the LKB1 tumor suppressor, STRAD alpha/beta and MO25 alpha/beta are upstream kinases in the AMP-activated protein kinase cascade. *J Biol* 2: 28.1–28.16, 2003.
17. **Hawley SA, Davison M, Woods A, Davies SP, Beri RK, Carling D, and Hardie DG.** Characterization of the AMP-activated protein kinase kinase from rat liver and identification of threonine 172 as the major site at which it phosphorylates AMP-activated protein kinase. *J Biol Chem* 271: 27879–27887, 1996.
18. **Hawley SA, Pan DA, Mustard KJ, Ross L, Bain J, Edelman AM, Frenguelli BG, and Hardie DG.** Calmodulin-dependent protein kinase kinase-beta is an alternative upstream kinase for AMP-activated protein kinase. *Cell Metab* 2: 9–19, 2005.
19. **Hawley SA, Selbert MA, Goldstein EG, Edelman AM, Carling D, and Hardie DG.** 5′ -AMP activates the AMP-activated protein kinase cascade, and Ca2+/calmodulin activates the calmodulin-dependent protein kinase I cascade, via three independent mechanisms. *J Biol Chem* 270: 27186–27191, 1995.
20. **Hayashi T, Hirshman MF, Fujii N, Habinowski SA, Witters LA, and Goodyear LJ.** Metabolic stress and altered glucose transport: activation of AMP-activated protein kinase as a unifying coupling mechanism. *Diabetes* 49: 527–531, 2000.
21. **Hayashi T, Hirshman MF, Kurth EJ, Winder WW, and Goodyear LJ.** Evidence for 5′ AMP-activated protein kinase mediation of the effect of muscle contraction on glucose transport. *Diabetes* 47: 1369–1373, 1998.
22. **Higaki Y, Hirshman MF, Fujii N, and Goodyear LJ.** Nitric oxide increases glucose uptake through a mechanism that is distinct from the insulin and contraction pathways in rat skeletal muscle. *Diabetes* 50: 241–247, 2001.
23. **Hurley RL, Anderson KA, Franzone JM, Kemp BE, Means AR, and Witters LA.** The Ca2+/calmodulin-dependent protein kinase kinases are AMP-activated protein kinase kinases. *J Biol Chem* 280: 29060–29066, 2005.
24. **Hurst D, Taylor EB, Cline TD, Greenwood LJ, Compton CL, Lamb JD, and Winder WW.** AMP-activated protein kinase kinase activity and phosphorylation of AMP-activated protein kinase in contracting muscle of sedentary and endurance-trained rats. *Am J Physiol Endocrinol Metab* 289: E710–E715, 2005.
25. **Hutber CA, Hardie DG, and Winder WW.** Electrical stimulation inactivates muscle acetyl-CoA carboxylase and increases AMP-activated protein kinase. *Am J Physiol Endocrinol Metab* 272: E262–E266, 1997.
26. **Ingebritsen TS, Lee HS, Parker RA, and Gibson DM.** Reversible modulation of the activities of both liver microsomal hydroxymethylglutaryl coenzyme A reductase and its inactivating enzyme. Evidence for regulation by phosphorylation-dephosphorylation. *Biochem Biophys Res Commun* 81: 1268–1277, 1978.
27. **Jorgensen SB, Viollet B, Andreelli F, Frosig C, Birk JB, Schjerling P, Vaulont S, Richter EA, and Wojtaszewski JF.** Knockout of the alpha2 but not alpha1 5′ -AMP-activated protein kinase isoform abolishes 5-aminoimidazole-4-carboxamide-1-beta-4-ribofuranoside but not contraction-induced glucose uptake in skeletal muscle. *J Biol Chem* 279: 1070–1079, 2004.

28. **Kemppainen J, Fujimoto T, Kalliokoski KK, Viljanen T, Nuutila P, and Knuuti J.** Myocardial and skeletal muscle glucose uptake during exercise in humans. *J Physiol* 542: 403–412, 2002.
29. **Langfort J, Viese M, Ploug T, and Dela F.** Time course of GLUT4 and AMPK protein expression in human skeletal muscle during one month of physical training. *Scand J Med Sci Sports* 13: 169–174, 2003.
30. **Lund S, Holman GD, Schmitz O, and Pedersen O.** Contraction stimulates translocation of glucose transporter GLUT4 in skeletal muscle through a mechanism distinct from that of insulin. *Proc Natl Acad Sci USA* 92: 5817–5821, 1995.
31. **McGee SL, Howlett KF, Starkie RL, Cameron-Smith D, Kemp BE, and Hargreaves M.** Exercise increases nuclear AMPK alpha2 in human skeletal muscle. *Diabetes* 52: 926–928, 2003.
32. **Minokoshi Y, Kim YB, Peroni OD, Fryer LG, Muller C, Carling D, and Kahn BB.** Leptin stimulates fatty-acid oxidation by activating AMP-activated protein kinase. *Nature* 415: 339–343, 2002.
33. **Moore F, Weekes J, and Hardie DG.** Evidence that AMP triggers phosphorylation as well as direct allosteric activation of rat liver AMP-activated protein kinase. A sensitive mechanism to protect the cell against ATP depletion. *Eur J Biochem* 199: 691–697, 1991.
34. **Mu J, Brozinick JT Jr, Valladares O, Bucan M, and Birnbaum MJ.** A role for AMP-activated protein kinase in contraction- and hypoxia-regulated glucose transport in skeletal muscle. *Mol Cell* 7: 1085–1094, 2001.
35. **Musi N, Hayashi T, Fujii N, Hirshman MF, Witters LA, and Goodyear LJ.** AMP-activated protein kinase activity and glucose uptake in rat skeletal muscle. *Am J Physiol Endocrinol Metab* 280: E677–E684, 2001.
36. **Nielsen JN, Mustard KJ, Graham DA, Yu H, MacDonald CS, Pilegaard H, Goodyear LJ, Hardie DG, Richter EA, and Wojtaszewski JF.** 5′ -AMP-activated protein kinase activity and subunit expression in exercise-trained human skeletal muscle. *J Appl Physiol* 94: 631–641, 2003.
37. **Park SH, Gammon SR, Knippers JD, Paulsen SR, Rubink DS, and Winder WW.** Phosphorylation-activity relationships of AMPK and acetyl-CoA carboxylase in muscle. *J Appl Physiol* 92: 2475–2482, 2002.
38. **Pold R, Jensen LS, Jessen N, Buhl ES, Schmitz O, Flyvbjerg A, Fujii N, Goodyear LJ, Gotfredsen CF, Brand CL, and Lund S.** Long-term AICAR administration and exercise prevents diabetes in ZDF rats. *Diabetes* 54: 928–934, 2005.
39. **Ponticos M, Lu QL, Morgan JE, Hardie DG, Partridge TA, and Carling D.** Dual regulation of the AMP-activated protein kinase provides a novel mechanism for the control of creatine kinase in skeletal muscle. *EMBO J* 17: 1688–1699, 1998.
40. **Sakamoto K, Goransson O, Hardie DG, and Alessi DR.** Activity of LKB1 and AMPK-related kinases in skeletal muscle: effects of contraction, phenformin, and AICAR. *Am J Physiol Endocrinol Metab* 287: E310–E317, 2004.
41. **Salt I, Celler JW, Hawley SA, Prescott A, Woods A, Carling D, and Hardie DG.** AMP-activated protein kinase: greater AMP dependence, and preferential nuclear localization, of complexes containing the alpha2 isoform. *Biochem J* 334: 177–187, 1998.
42. **Stapleton D, Mitchelhill KI, Gao G, Widmer J, Michell BJ, Teh T, House CM, Fernandez CS, Cox T, Witters LA, and Kemp BE.** Mammalian AMP-activated protein kinase subfamily. *J Biol Chem* 271: 611–614, 1996.
43. **Stein SC, Woods A, Jones NA, Davison MD, and Carling D.** The regulation of AMP-activated protein kinase by phosphorylation. *Biochem J* 345: 437–443, 2000.
44. **Stephens TJ, Chen ZP, Canny BJ, Michell BJ, Kemp BE, and McConell GK.** Progressive increase in human skeletal muscle AMPKalpha2 activity and ACC phosphorylation during exercise. *Am J Physiol Endocrinol Metab* 282: E688–E694, 2002.
45. **Toyoda T, Hayashi T, Miyamoto L, Yonemitsu S, Nakano M, Tanaka S, Ebihara K, Masuzaki H, Hosoda K, Inoue G, Otaka A, Sato K, Fushiki T, and Nakao K.** Possible involvement of the α1-isoform of 5′ -AMP-activated protein kinase in oxidative stress-stimulated glucose transport in skeletal muscle. *Am J Physiol Endocrinol Metab* 287: E166–E173, 2004.
46. **Vavvas D, Apazidis A, Saha AK, Gamble J, Patel A, Kemp BE, Witters LA, and Ruderman NB.** Contraction-induced changes in acetyl-CoA carboxylase and 5′ -AMP-activated kinase in skeletal muscle. *J Biol Chem* 272: 13255–13261, 1997.
47. **Weekes J, Hawley SA, Corton J, Shugar D, and Hardie DG.** Activation of rat liver AMP-activated protein kinase by kinase kinase in a purified, reconstituted system. Effects of AMP and AMP analogues. *Eur J Biochem* 219: 751–757, 1994.
48. **Winder WW, Hardie DG, Mustard KJ, Greenwood LJ, Paxton BE, Park SH, Rubink DS, and Taylor EB.** Long-term regulation of AMP-activated protein kinase and acetyl-CoA carboxylase in skeletal muscle. *Biochem Soc Trans* 31: 182–185, 2003.
49. **Winder WW, Wilson HA, Hardie DG, Rasmussen BB, Hutber CA, Call GB, Clayton RD, Conley LM, Yoon S, and Zhou B.** Phosphorylation of rat muscle acetyl-CoA carboxylase by AMP-activated protein kinase and protein kinase A. *J Appl Physiol* 82: 219–225, 1997.
50. **Wojtaszewski JF, Nielsen P, Hansen BF, Richter EA, and Kiens B.** Isoform-specific and exercise intensity-dependent activation of 5′ -AMP-activated protein kinase in human skeletal muscle. *J Physiol* 528: 221–226, 2000.
51. **Zou MH, Hou XY, Shi CM, Kirkpatick S, Liu F, Goldman MH, and Cohen RA.** Activation of 5′ -AMP-activated kinase is mediated through c-Src and phosphoinositide 3-kinase activity during hypoxia-reoxygenation of bovine aortic endothelial cells. Role of peroxynitrite. *J Biol Chem* 278: 34003–34010, 2003.

Available online at www.sciencedirect.com
SCIENCE DIRECT®
ELSEVIER
Diabetes Research and Clinical Practice 71 (2006) 227–232
DIABETES RESEARCH AND CLINICAL PRACTICE
www.elsevier.com/locate/diabres

A case of type 2 diabetes mellitus developing hypothyroidism discovered as a result of a discrepancy between glycated hemoglobin and glycated albumin values

Kenji Moriyama *, Naotetsu Kanamoto, Yuji Hataya, Takuo Nanbu, Kiminori Hosoda, Hiroshi Arai, Kazuwa Nakao

Department of Endocrinology and Metabolism, School of Medicine, Kyoto University, 54 Kawahara-cho, Shogoin, Sakyo-ku, Kyoto, 606-8705 Japan

Received 24 March 2005; received in revised form 6 June 2005; accepted 28 June 2005
Available online 19 August 2005

Abstract

We report a case of type 2 diabetes mellitus presenting hypothyroidism due to overeating of seaweed that was noticed as a result of a discrepancy between glycated albumin (GA) and glycated hemoglobin (GHb). A 71-year-old woman was undergoing managed treatment with oral medicines and insulin for diabetes mellitus with no sign of thyroid disease. Her thyroid function was euthyroid without aid of thyroid hormone. All of the patient's thyroid autoantibodies were negative. Fifteen weeks prior to indications of hypothyroidism, she had started to consume large amounts (100–200 g dry weight equivalent) of cooked "wakame" seaweed every morning. Just before admission to our hospital, her GA was 26.9%, while GHb and fasting plasma glucose remained within normal ranges (less than 5.6%, and 106 mg, respectively). This discrepancy between GA and GHb drew our attention to the development of complications. Naive interview of the patient led us to believe a thyroid hormone deficiency existed, though without any related complaints or findings, such as non-pitting edema, cold intolerance, or easy fatiguing. Seaweed consumption was stopped and periodic observation of thyroid function started. As thyroid hormone levels moved into normal range, GA and GHb returned to their normal relative ratio after 3 months. Thus, measurement of the relative ratio of GA and GHb may be useful for glycemic monitoring, with the potential as a readily available glycemic control marker for patients with changeable complications.

Keywords: Glycated albumin; Glycated hemoglobin; Seaweed; Hypothyroidism

1. Introduction

Measurement of glycated hemoglobin (GHb) and hemoglobin A1c is now well established as the best means of measuring overall glucose control in

* Corresponding author. Tel.: +81 75 751 3181; fax: +81 75 771 9452.
E-mail address: kemori@kuhp.kyoto-u.ac.jp (K. Moriyama).

0168-8227/$ – see front matter © 2005 Elsevier Ireland Ltd. All rights reserved.
doi:10.1016/j.diabres.2005.06.013

managing diabetes. Other glycated serum protein assays reflecting recent glycemic control, e.g., glycated albumin (GA) and fructosamine, have also been validated in recent clinical studies. Measurement of plasma concentrations of GA has been widely adopted and opportunities for examination are gradually increasing. Chronic hyperglycemia in diabetes results in increased concentrations of glycated proteins including GHb and GA [1–3]. Since the modification of hemoglobin by glucose occurs continually during the life span of the erythrocyte, GHb concentrations provide a time-average index of the degree of hyperglycemia during the previous 2 months in humans. In the same way, GA appears to provide an index of the state of glycemic control for approximately the previous 2 weeks.

In clinical management of diabetic patients with various complications, GA provides valuable information for the control of blood glucose. Under several conditions, notably in type 1 diabetes initial treatment periods, in gestational diabetic patients, and for diabetes with chronic renal failure, GA is regarded as a primary index of glycemic control rather than GHb and/or blood glucose.

Discrepancies in the normal relative ratio of GA and GHb have been reported in cases of thyroid function disorders, liver cirrhosis, mal-nutrition, nephritic syndrome, burning, and bleeding. Such discrepancies have been attributed mostly to changes in the half-life of serum albumin.

However, we have found no previous clinical report on the relative relationship between GA and GHb, and thyroid function disorders. We present here the first reported clinical case of a type 2 diabetic patient with hypothyroidism in which we observed characteristic changes in concentrations of both GA and GHb in her clinical course.

2. Case report

A 71-year-old woman, suffering from type 2 diabetes mellitus since 1981, was admitted to our hospital on November 6, 2002. The 2 weeks before admission she had suffered from dull chest pain. She was then admitted for further examination of her cardiovascular system and diabetes-related complications.

Her height was 158 cm and weight 56.4 kg. Blood pressure was 134/72 mmHg; pulse rate, 65 beats per minute; temperature, 36.4 °C. There was no family history of diabetes mellitus. During a hysterectomy due to a myoma uterus in 1981 she received no blood transfusion. The patient had diabetic neuropathy, diabetic retinopathy and cataract, but no diabetic nephropathy. Her thyroid gland was of normal size and consistency. There were no remarkable findings in the liver, lungs, and chest. We noted a surgical hysterectomy scar on the abdomen.

The patient's laboratory data on admission is shown in Table 1. Urinalysis, including proteinuria and glucosuria by dipstick, showed no abnormalities. Urine albumin concentration was 16.0 mg/24 h, within normal levels based on American Diabetes Association: Position statement; Diabetic nephropathy (Diabetes Care 22 (Suppl. 1) (1999) S66–S69). Concentrations of total protein and total bilirubin, serum enzyme levels, such as serum asparate aminotransferase (AST) and alanine aminotransferase (ALT), alkaline phosphatase, lactate dehydrogenase (LDH), and levels of blood urea nitrogen and creatinine were within normal ranges. However, hemoglobin concentration, hematocrit and platelets were a little low, being 10.4 g/dL, 30.6%, and 15.1×10^4 mm^{-3}, respectively. There were no remarkable findings in serum ions. Fasting plasma glucose and GHb were 106 mg/dL and 5.6%, respectively. C-peptide immunoreactivity in urine was less than 42 μg/day. HCV antibody, hepatitis B (HB) surface antigen and anti-HB core antibody in serum were negative. Circulating autoantibodies to thyroid peroxidase (TPOAb) or thyroglobulin (TgAb) were not detectable. Anti-thyroid stimulating hormone (TSH) receptor antibody was negative, as were anti-nuclear antibody (ANA), anti-DNA antibody, and rheumatoid factor (RF).

2.1. Clinical course of the patient

The patient's diabetes had been initially controlled at the time of admission with Novolin 70/30® 18U, metformin–HCl 750 mg. Nitrendipine 10 mg and asprin 81 mg were also administered for essential hypertension and the prevention of microembolism. Her blood sugar profiles on the 2nd day of admission were 106-140-113-148 mg/dL, respectively, for each meal and before sleep, and her average FBS over the 6-month period prior to admission was 98.00 ± 17.98 mg/dL (average of 6 times ± S.D.) with no remarkable

Table 1
Laboratory findings

		References
CBC		
WBC	3800 mm^{-3}	(2800–9300)
RBC	314 × 10^4 mm^{-3}	(319–482)
HGB	10.4 g/dL	(10.2–14.6)
HCT	30.6%	(29.8–43.4)
PLT	15.1 × 10^4 mm^{-3}	(12.3–34.3)
RET	19.6 promil	(7.0–20.0)
RF	–	
Blood chemistry		
AST	28 IU/L	(13–29)
ALT	23 IU/L	(8–28)
LDH	227 IU/L	(129–241)
ALP	98 IU/L	(118–335)
G-GTP	15 IU/L	(7–29)
LAP	53 IU/L	(37–65)
TP	6.8 g/dL	(6.3–8.1)
ALB	3.9 g/dL	(3.9–5.1)
CH-E	183 IU/L	(201–436)
T-BIL	0.8 mg/dL	(0.2–1.0)
CRE	0.7 mg/dL	(0.4–0.8)
UA	4 mg/dL	(3.6–7.8)
BUN	10 mg/dL	(8–22)
Glucose	106 mg/dL	(65–105)
HbAlc	5.7%	(4.3–5.8)
T-CHO	181 mg/dL	(146–220)
LDL-CHO	104 mg/dL	(<140)
TG	70 mg/dL	(34–173)
CPK	151 IU/L	(35–141)
AMY	64 IU/L	(36–129)
Na	141 mEq/dL	(136–144)
K	3.5 mEq/dL	(3.6–4.8)
Cl	105 mEq/dL	(99–109)
Ca	8.4 mg/dL	(8.5–9.9)
P	3.7 mg/dL	(2.6–4.5)
Thyroid function		
TSH	>50 μIU/mL	(0.41–4.0)
Free T4	0.34 ng/dL	(0.82–1.63)
FreeT3	3.31 pg/dL	(2.00–4.90)
Urinalysis		
Proetine	–	
Glucose	–	
Blood	–	
β2MG	0	
Albumin	16.0 mg/24 h	(0–22.0)

changes. We also monitored both GA (Lucika GA ELISA kit, which employes enzymatic methodology with ketoamin oxidase, Asahi Kasei Corporation, Shizuoka, Japan) and GHb (using high-pressure liquid chromatography with a normal range of 4.0–5.8%) for short and long term blood glucose control, and her condition was thereafter monitored using these two control indices. On admission, the patient's GHb was 5.6%, while GA had increased to 26.9%, before any re-evaluation of the cardiovascular system.

The patient was diagnosed as having hypothyroidism due to undetermined reasons. Changes in serum diabetic control indices and endocrinological parameters of the thyroid gland after admission, such as TSH, free T4, and free T3, are shown in Fig. 1. Serum TSH was found to have risen off the scale (>50 μU/mL), accompanied by a lowering of free T4 to 0.34 ng/dL. The patient had been regularly eating seaweed 100–200 g/day (equivalent to dry weight), containing approximately 80–120 mg iodine, for the 4 months before admission. After she stopped eating seaweed, the level of GA somewhat declined together with that of TSH, and free T4 increased. However, GHb remained within normal limits despite the elevated TSH and GA levels (Fig. 1). From June 2003, the patient's body weight gradually increased, possibly due to lack of exercise. With the increase in body weight, both diabetic control indicators rose together in a parallel fashion, and the diabetic condition was controlled, with a GA of 25% and a GHb of 6.7%. These increases may have been due to unstable glycemic control or a reflection of postprandial hyperglycemia.

3. Discussion

We report here a case of a diabetic patient with non-autoimmune primary hypothyroidism. In our patient's case, ICA, anti-GAD antibody and IA in her history of diabetes were negative. Her fasting plasma glucose and GHb were normal and GA was mildly elevated just before ceasing her intake of seaweed. Ultrasound examinations of the thyroid gland revealed almost normal thyroid pattern without lymph node swelling (data not shown). Her estimated daily iodine intake was approximately 80–120 mg, almost 300–1000 times the Recommended Dietary Allowance for adult men and women (RDA, RDA has been recommended by WHO/International Council for the Control of Iodine/UNICEF), and 80–120 times greater than The Tolerable Upper Intake Level (UL) for adults (1.1 mg/day) [4]. The patient's thyroid function was not treated after admission with thyroid hormone as the hypothyroidism was believed to be a result of the

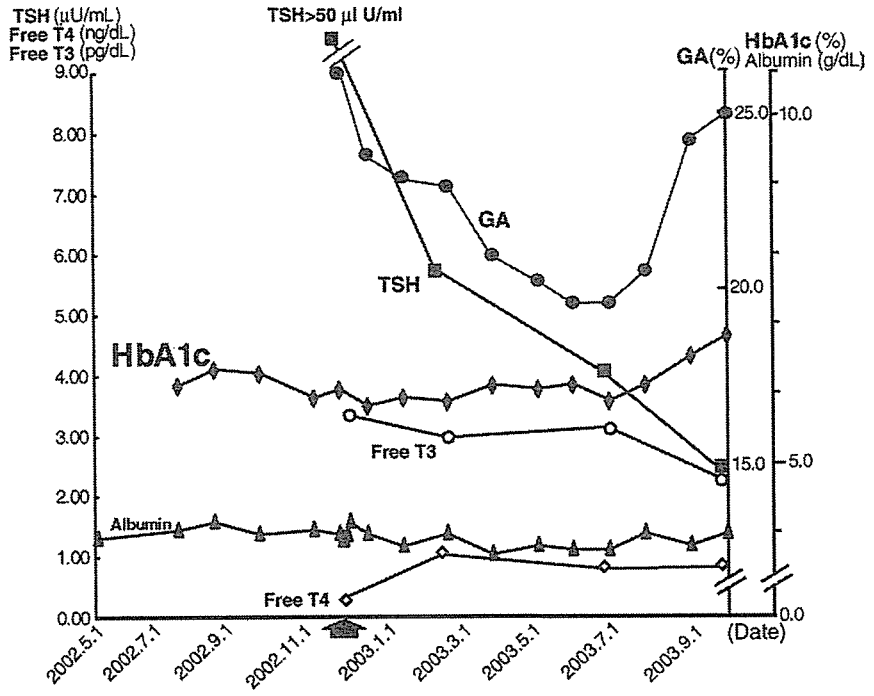

Fig. 1. Clinical course of the patient. Clinical course of serum GA, GHb, albumin, TSH, free T3 and free T4 are shown as solid circle, solid rhombus, solid triangle, solid square, open circle, and open rhombus, respectively. Left ordinate line indicates pg/dL for free T3, ng/mL for free T4, and μU/mL for TSH. Outer right ordinate line indicates % for GHb and mg/dL for albumin. Inner right ordinate line indicates % for GA. Abscissa line indicates time in date. Vertical arrow indicates admission to Kyoto University Hospital.

excessive ingested iodine, due to a prolonged Wolff–Chaikoff effect—the inhibition of organification of iodide in the thyroid [5]. Serum TSH levels measured in the initial course of the episode were clearly elevated, and then normalized after the eating of seaweed stopped, in parallel with the decline in serum GA levels. When the thyroid hormone level returned to normal, the GA value had been gradually decreasing. These findings suggest that impaired thyroid function resulting in elevation of GA levels played a principal role in the development of the discrepancy in the GA and GHb ratio found in our patient. We surmised that the false positive GA increase started with her over-consumption of seaweed as there no symptoms, signs or laboratory findings, such as non-pitting edema or hypercholesteremia.

These two glycemic markers, GA and GHb, have a tendency to track the other, though the normal range of variation in the GA–GHb ratio has yet to be determined. In the latter part of 2003, our patient's GA–GHb ratio was within the predictable theoretical limits, ranging between 1:3 and 1:4, suggesting that her hemoglobin was not defective. Although hemoglobin interferes with measurement of GA, we did not use hemolyzed samples. We found no other factors except hypothyroidism that might have affected blood glucose and/or glycated protein control, nor did we note any other complication that would disrupt the metabolic ratio of serum albumin, such as liver cirrhosis or renal insufficiency. In view of this, it is likely glycosylation resulted in accumulated albumin with delayed turnover periods and thus a false elevated GA value rather than false-negative GHb.

Non-enzymatic glycation is a universal process affecting serum and intracellular proteins, providing the half-life of these proteins is sufficient for the glycation reaction to proceed beyond Schiff base formation [6]. The most accessible example of these proteins for measurement is a circulating pool in the serum of which albumin is the most abundant.

Albumin glycation accounts for as much as 90% of total measured serum protein glycation [7]. Interest in possible uses of glycated albumin or other glycated serum proteins has been developing for some time [8–10]. The potential advantage of measuring such proteins is that they may provide a more suitable index to reflect changes in hyperglycemia over shorter periods of time than does GHb [9,10]. If the metabolic rate of albumin is stable, GA appears to provide an index of the state of glycemic control for approximately the previous 2–3 weeks. However, if the serum albumin level changes, the metabolic rate of the albumin will vary. Parving and Rossing have reported on metabolic turnover of ^{131}I-labeled albumin in normal and pathophysiological states, such as primary myxedema. In their study, seven hypothyroid patients presented prolonged turnover rates of albumin: 153–207 μmol/24 h, before and after treatment with L-thyroxine, respectively [11]. In contrast, GHb testing is affected by co-morbid illnesses; there are a number of potential pitfalls in the use of such tests in the presence of a hemoglobinopathy or other complicated illness. In some clinical situations, certain methods offer better insight into glycemic control than others. Hemolytic anemia, HbS, HbC, acute or chronic blood loss, and pregnancy have produced false lower results for the glycated fraction [12].

Thyroid hormones are involved in various metabolic reactions and metabolic ratios, possibly attributable to both synthesis and degradation of albumin, although there have been no reports describing exact metabolic ratios. Hypothyroid rats treated with 2-mercapto-1-methylimidazole (methimazole) showed a slight increase in albumin levels. Hyperthyroid rats given daily injections of thyroxin showed significant augmentation of serum albumin concentrations [13]. Our patient's albumin level remained stable in the course of this episode (Fig. 1).

Discrepancies between GA and GHb have been observed in certain patients with non-insulin-dependent diabetes mellitus and also suffering from thyroid function disorders, liver cirrhosis, mal-nutrition, nephritic syndrome, burning, or bleeding. However, there are still a small number of patients in whom GA and GHb values are in discord with those predicted at the managed phase. The pathophysiological reasons for such variations from the norm are not yet fully understood.

GA levels generally correlate well with GHb values in an individual. However, in our case, GA could not be inferred with any reliability from the level of GHb, nor could the change in GHb be inferred from the change in GA. We suggest that if GHb is to be used as a regular index of glycemic control in diabetes, it should be supplemented by measurement of GA when glycemic controls are not stable or at the initial consultation for diabetes, to determine whether the GHb and GA values are consistent with glycemic control targets for that individual.

References

[1] F.H. Bunn, H.K. Gabby, M.P. Gallop, The glycosylation of hemoglobin: relevance to diabetes mellitus, Science 20 (1978) 21–27.
[2] J.F. Day, S.R. Thorpe, J. Baynes, Non-enzymatic glycosylation of rat serum proteins in vitro and in vivo, Fed. Proc. 38 (1979) 418.
[3] J.M. McDonald, J.E. Davis, Glycosylation of serum albumin: elevated glycosyl-albumin in diabetic patients, FEBS Lett. 103 (1979) 282–286.
[4] Food and Nutrition Board, Institute of Medicine, Iodine, in: Dietary Reference Intakes for Vitamin A, Vitamin K, Arsenic, Boron, Chromium, Copper, Iodine, Iron, Manganese, Molybdenum, Nickel, Silicon, Vanadium, and Zinc, The National Academic Press, Washington, DC, 2000, pp. 258–289.
[5] U. Bando, Y. Ushiogi, D. Toya, N. Tanaka, M. Fujisawa, Diabetic nephropathy accompanied by iodine-induced non-autoimmune primary hypothyroidism: two case reports, Endocr. J. 46 (1999) 803–810.
[6] K.G.M.M. Alberti, P. Zimmet, R.A. Defronzo, Glycation of serum proteins, in: International Textbook of Diabetes Mellitus, second ed., John Wiley & Sons Ltd., England, 1997.
[7] R. Dolhofer, O.H. Wieland, Glycosylation of serum albumin: elevated glycosyl-albumin in diabetic patients, FEBS Lett. 103 (1979) 282–286.
[8] C.E. Guthrow, M.A. Morris, J.F. Day, S.R. Thorpe, J.W. Baynes, Enhanced nonenzymatic glucosylation of human serum albumin in diabetes mellitus, Proc. Natl. Acad. Sci. U.S.A. 76 (1979) 4258–4261.
[9] A.L. Kennedy, T.J. Merimee, Glycosylated serum protein and hemoglobin A1 levels to measure control of glycemia, Ann. Intern. Med. 95 (1981) 56–58.
[10] M. Rendell, R. Paulsen, S. Eastberg, P.M. Stephen, J.L. Valentine, C.H. Smith, et al. Clinical use and time relationship of changes in affinity measurement of glycosylated albumin and glycosylated hemoglobin, Am. J. Med. Sci. 292 (1986) 11–14.
[11] H.H. Parving, J.M. Hansen, S.L. Nielsen, N. Rossing, O. Munck, N.A. Lassen, Mechanism of edema formation in myxedema-increased protein extravasation and relatively slow lymphatic drainage, N. Engl. J. Med. Jpn. J. Med. 301 (1979) 460–465.

[12] C. Eberentz-Lhomme, R. Ducrocq, S. Intrator, J. Elion, E. Nunez, R. Assan, Haemoglobinopathies: a pitfall in the assessment of glycosylated haemoglobin by ion-exchange chromatography, Diabetologia 27 (1984) 596–598.

[13] J. Naval, M. Calvo, F. Lampreave, A. Pineiro, Thyroxine-induced changes in the glycosylation pattern and in brain and serum levels of rat alpha-fetoprotein, Int. J. Biochem. 18 (1986) 115–122.

Nephrol Dial Transplant (2006) 21: 2472–2477
doi:10.1093/ndt/gfl260
Advance Access publication 4 July 2006

Original Article

NDT
Nephrology Dialysis Transplantation

Redistribution of connexin43 expression in glomerular podocytes predicts poor renal prognosis in patients with type 2 diabetes and overt nephropathy

Kazutomo Sawai[1], Masashi Mukoyama[1], Kiyoshi Mori[1], Hideki Yokoi[1], Masao Koshikawa[1], Tetsuro Yoshioka[1], Ryuji Takeda[2], Akira Sugawara[1], Takashi Kuwahara[3], Moin A. Saleem[4], Osamu Ogawa[5] and Kazuwa Nakao[1]

[1]Department of Medicine and Clinical Science, Kyoto University Graduate School of Medicine, Kyoto, [2]Department of Life Science and Chemistry, Kinki University Graduate School of Agriculture, Nara, [3]Department of Nephrology, Osaka Saiseikai Nakatsu Hospital, Osaka, Japan, [4]Children's Renal Unit, University of Bristol, Bristol, UK and [5]Department of Urology, Kyoto University Graduate School of Medicine, Kyoto, Japan

Abstract

Background. Significance of podocyte injury in the progression of diabetic nephropathy is not well-understood. In this study, we examined whether alteration of gap junction protein connexin43 (Cx43) expression in podocytes is associated with the progression of overt diabetic nephropathy.

Methods. We recruited 29 type 2 diabetic patients with overt nephropathy who underwent renal biopsy. Nephrectomized kidney samples obtained from seven subjects with localized neoplasm and biopsy specimens from five patients diagnosed as minor glomerular abnormalities were used as controls. Cx43 staining on paraffin-embedded kidney sections were studied by immunohistochemistry.

Results. In controls, Cx43 was expressed at podocytes in a linear pattern along the glomerular basement membrane. In contrast, downregulation and loss of uniformly linear staining of Cx43 (Cx43 heterogeneity) in podocytes were observed in diabetic nephropathy. Cx43 intensity correlated with current renal function ($R=0.647$, $P<0.005$), whereas the magnitude of Cx43 heterogeneity correlated well with the degree of future decline in renal function ($R=-0.705$, $P<0.001$).

Conclusions. Alteration of Cx43 expression in podocytes was closely associated with the progression of overt diabetic nephropathy. These results indicate that change in Cx43 expression at podocytes represents a progressive stage in overt diabetic nephropathy and that it may be a convenient way to predict future decline in renal function.

Correspondence and offprint requests to: Dr Masashi Mukoyama, Department of Medicine and Clinical Science, Kyoto University Graduate School of Medicine, 54 Shogoin Kawahara-cho, Sakyo-ku, Kyoto 606-8507, Japan. Email: muko@kuhp.kyoto-u.ac.jp

Keywords: connexin43; glomerular visceral epithelial cell; overt diabetic nephropathy; pathogenesis; podocyte; prognosis

Introduction

Podocytes are highly differentiated glomerular cells crucially involved in establishing selective permeability properties of the glomerular filtration barrier. Injury to podocytes leads to proteinuria, a hallmark of most glomerular diseases [1]. Decline in renal function in renal diseases is due to the progressive loss of viable nephrons. In majority of cases, the loss of nephrons most likely starts with the injury of podocytes [1]. Recent studies have revealed that podocyte loss or decrease in podocyte density is an early event in diabetic nephropathy [2], and that podocyte number predicts long-term urinary albumin excretion [3]. Podocyte loss in animal models of diabetic nephropathy is also reported [4]. These results suggest that podocyte injury is implicated in the pathogenesis of diabetic nephropathy, but the role of podocytes in the progression of diabetic nephropathy is not well-understood.

The rate of decline in glomerular function in overt diabetic nephropathy is highly variable from individual to individual with type 1 and type 2 diabetes [5]. Early identification of patients with progressive diabetic nephropathy is of great value, since such patients are in need for an intensified therapeutic regimen. A growing body of information supports the view that risk factors for diabetic nephropathy may be intrinsic to the kidney [5]. This notion is supported by the fact that there is a marked variability in the rate of development of kidney lesions of diabetic nephropathy